Computerized Medical Imaging and Graphics 108 (2023) 102274

Contents lists available at ScienceDirect

Computerized Medical Imaging and Graphics

journal homepage: www.elsevier.com/locate/compmedimag

Graph neural network based unsupervised influential sample selection for brain multigraph population fusion

Mert Can Kurucu [a,b], Islem Rekik [a,*,1], for the Alzheimer's Disease Neuroimaging Initiative

[a] BASIRA Lab, Imperial-X and Computing Department, Imperial College London, London, UK
[b] Istanbul Technical University, Istanbul, Turkey

ARTICLE INFO

Keywords:
Graph neural networks
Sample selection
Multigraph population fusion
Unsupervised learning
Connectional brain templates

ABSTRACT

Graph neural networks (GNNs) have witnessed remarkable proliferation due to the increasing number of applications where data is represented as graphs. GNN-based multigraph population fusion methods for estimating population representative connectional brain templates (CBT) have recently led to improvements, especially in network neuroscience. However, prior studies do not consider how an individual training brain multigraph influences the quality of GNN training for brain multigraph population fusion. To address this issue, we propose two major sample selection methods to quantify the *influence* of a training brain multigraph on the brain multigraph population fusion task using GNNs, in ***a fully unsupervised manner***: (1) *GraphGradIn*, in which we use gradients w.r.t GNN weights to trace changes in the centeredness loss of connectional brain template during the *training phase*; (2) *GraphTestIn*, in which we exclude a training brain multigraph of interest during the refinement process in the *test phase* to infer its influence on the CBT centeredness loss. Next, we select the most influential multigraphs to build the training set for brain multigraph population fusion into a CBT. We conducted extensive experiments on brain multigraph datasets to show that using a dataset of influential training samples improves the learned connectional brain template in terms of centeredness, discriminativeness, and topological soundness. Finally, we demonstrate the use of our methods by discovering the connectional fingerprints of healthy and neurologically disordered brain multigraph populations including Alzheimer's disease and Autism spectrum disorder patients. Our source code is available at https://github.com/basiralab/GraphGradIn.

1. Introduction

Deep learning (DL) has revolutionized many fields that deal with Euclidean data, from speech recognition (Hinton et al., 2012) and machine translation (Sutskever et al., 2014) to image analysis and computer vision (Taigman et al., 2014). The use of graphs to represent non-Euclidean data with complex relationships has recently grown, particularly in network neuroscience (He and Evans, 2010; van den Heuvel and Sporns, 2019). With the proliferation of large-scale neuroimaging datasets using non-invasive magnetic resonance imaging (MRI), our understanding of the exceptionally complex yet topologically organized nature of the human neural architecture (i.e., connectome) has significantly improved (Sporns, 2012; Van Essen and Glasser, 2016). Leveraging these multi-modal data sources allows for a comprehensive representation of the human brain network using multigraphs. In this model, individual nodes correspond to specific brain regions, and multiple edges between a pair of nodes signify various interactions between the respective brain regions (De Vico Fallani et al., 2014; Mahjoub et al., 2018; Lisowska and Rekik, 2019).

Such network-centered perspective has provided a basis for understanding the functional integration, segregation, resilience, or organization of the brain network as a whole or the individual brain regions of interest (ROI) of the healthy and disordered brain (Bullmore and Bassett, 2011; Reijneveld et al., 2007). The application of traditional DL frameworks to graphs does not lead to satisfactory results due to their inability to take advantage of the topological properties of such non-Euclidean data (Bronstein et al., 2017; Henaff et al., 2015). To overcome this limitation, an extended family of DL methods dealing with non-Euclidian data, namely graph neural networks (GNNs) have been proposed as an alternative to traditional DL algorithms in many fields (Monti et al., 2016; Wang et al., 2020; Zhang et al., 2022) including the field of network neuroscience (Bessadok et al., 2021; Wang et al., 2021). GNNs demonstrate significant potential in capturing

* Corresponding author.
E-mail address: i.rekik@imperial.ac.uk (I. Rekik).
[1] http://basira-lab.com/, GitHub code: https://github.com/basiralab/GraphGradIn.

https://doi.org/10.1016/j.compmedimag.2023.102274
Received 27 February 2023; Received in revised form 17 July 2023; Accepted 17 July 2023
Available online 21 July 2023

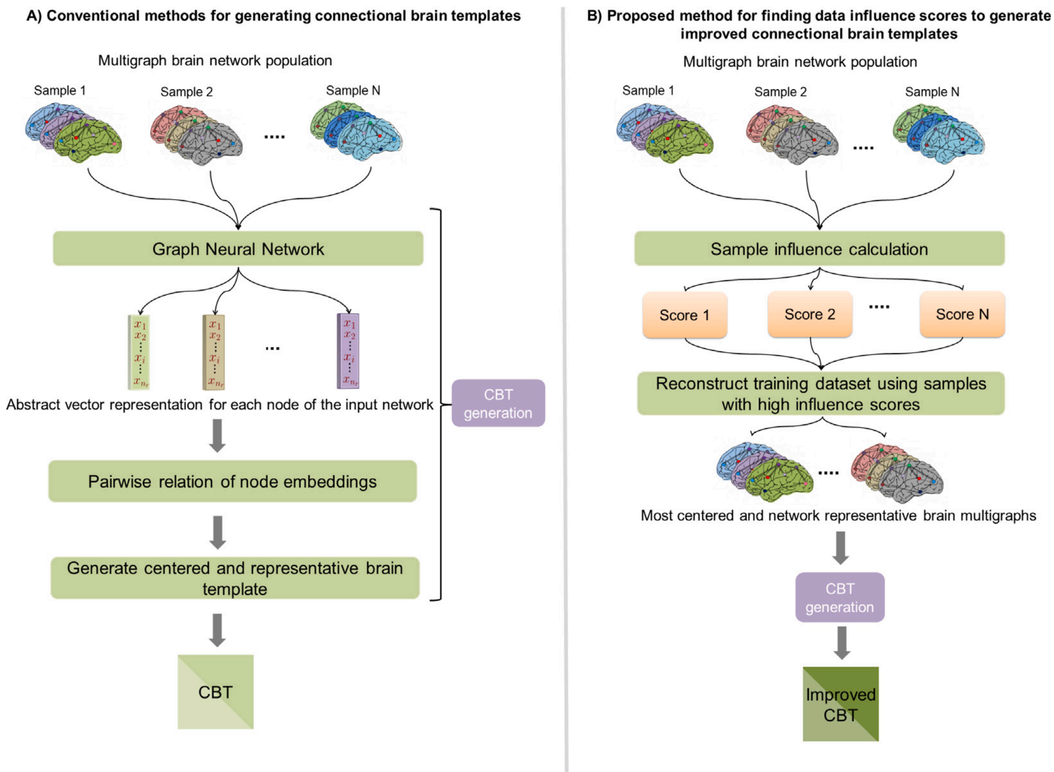

Fig. 1. **(A)** Conventional CBT estimation methods use whole training dataset for multigraph population integration. **(B)** Our proposed framework calculates influence scores and selects the most influential brain multigraphs in improving the population template learned in terms of representativeness, discriminativeness, and topological soundness.

the topological properties of graphs, thereby enhancing performance in tasks such as classification or regression (Wu et al., 2021).

Fusing a heterogeneous population of brain multigraphs to produce a connectional brain template (CBT) that characterizes the unique features of that population is a crucial step for group comparison studies (Rekik et al., 2017; Dhifallah and Rekik, 2020). Moreover, this CBT can be used for brain graph classification as well as evolution prediction (Bessadok et al., 2021; Gürler et al., 2020). Recently introduced machine learning and GNN-based methods have significantly improved the performance of integrating a heterogeneous brain multigraph population in terms of well-centeredness, discriminativeness, topological soundness (Gurbuz and Rekik, 2020; Burak Gürbüz and Rekik, 2021) and even predicting its temporal evolution (Demirbilek and Rekik, 2021). However, these studies do not investigate how each training brain multigraph influences the quality of the GNN-based CBT generation. In fact, a particular brain multigraph in the population may capture the essence of the population traits better and positively influence the learning of the population-driven CBT. The success of machine learning and deep learning models is closely tied to the quality and volume of the training data. However, clinical datasets often contain few samples due to the limited availability of physicians and the time-intensive pre-processing pipeline for a single raw MRI. We hypothesize that optimally choosing a training subset from the entire dataset in a fully unsupervised manner is critical for learning well-centered, representative, and topologically sound connectional brain templates. Without any loss of generalizability, this line of reasoning extends to any set of training data represented by multigraphs.

1.1. Related work

Multigraph population fusion methods. The process of normalizing or integrating brain networks is a challenging task, largely due to the variation in brain connectivity across individuals, which restricts our ability to disentangle the typical brain connectional variation from the atypical one (Bullmore and Sporns, 2009; Bullmore and Bassett, 2011). Reducing inter-subject variation in both healthy and disordered populations through the brain multigraph population integration process better spots the 'pathological' changes in brain connectivities as deviations from a 'standardized/normalized' brain network representation (Dhifallah and Rekik, 2020; Burak Gürbüz and Rekik, 2021; Gürler et al., 2020). Network fusion studies introduced the term connectional brain template (CBT) as an integrated connectional fingerprint of the brain multigraph population (Rekik et al., 2017).

For the integration of a population of networks, Wang et al. (2014) proposed a non-linear network integration technique, namely similarity network fusion (SNF), which aims to estimate a status matrix for each network and a sparse local matrix that takes the top-k neighbors into account. Next, an iterative integration step is carried out to update each status network using the mean global structure of the remaining networks and the sparse local network. Although SNF is a powerful graph integration method, it comes with strong assumptions such as emphasizing the best k local connections for each node and evenly averaging the global topology of individual networks at each iterative update. Another method proposed by Dhifallah and Rekik (2020), is called netNorm, which first creates a high-order graph using the cross-view connection properties as nodes and their Euclidean distance between the cross-view feature vectors across all subjects as a measure of dissimilarity. Next, netNorm selects the most centered cross-view feature vectors in the population. Finally, the network views are integrated into a single network using a non-linear fusion technique to output the final connectional brain template. While this method produces satisfactory results, it uses Euclidean distance between the cross-view feature vectors across all subjects as a predefined metric, which might potentially fail to capture non-linear patterns in the brain multigraph population. Additionally, netNorm consists of independent feature extraction, feature selection, and fusion steps. These fully independent steps cannot provide feedback to each other in order to globally optimize the template estimation process.

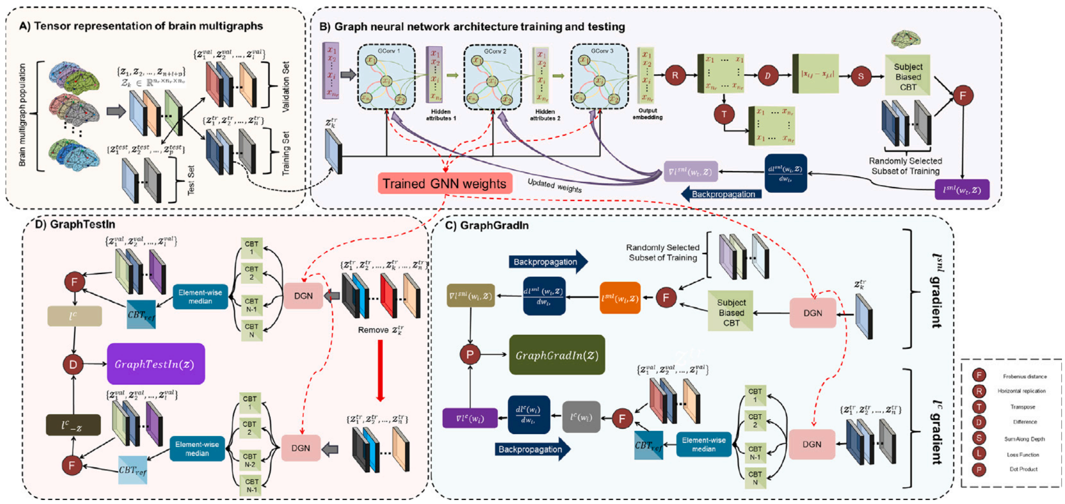

Fig. 2. *Proposed unsupervised training sample influence quantification for brain multigraph integration.* **(A) Tensor representation of brain multigraph networks.** Each brain multigraph sample is represented by $\mathcal{Z}_k \in \mathbb{R}^{n_r \times n_r \times n_v}$, composed of an undirected fully-connected graph. **(B) Graph neural network architecture.** DGN embeds connectivity patterns onto a high-dimensional vector representation for each node in each brain multigraph data. For each graph convolution layer and for each brain multigraph connection e_{ij} linking node i and j, we create an edge-specific weight matrix using an edge-conditioned filter learner. **(C) *GraphGradIn*.** We use gradients w.r.t weights of GNN, taken from the trained model in section (B), to approximate how much a training data point influences the CBT centeredness loss ℓ^c to acquire the influence score of a training point $\mathcal{Z}$ during the *training phase*. **(D) *GraphTestIn*.** we exclude a training brain multigraph of interest $\mathcal{Z}$ during the CBT refinement step in the *test phase* using the trained model in section (B), to trace the change in centeredness loss. In both GraphGradIn and GraphTestIn, we use validation data to calculate the loss to ensure that the test dataset remains untouched.

Recently, a novel graph neural network structure named Deep Graph Normalizer (DGN) was introduced in Gurbuz and Rekik (2020). This leading work on CBT learning leveraged the power of geometric deep learning for multigraph integration, producing significant improvements in estimating well-representative, centered, and topologically sound CBTs. Despite its promising results, DGN does not directly consider the topological correctness of learned CBT. Burak Gürbüz and Rekik (2021), which is an extension of Gurbuz and Rekik (2020), proposed a novel loss function that penalizes the deviation from the ground-truth node strength topological distribution, thereby preserving the topology of the input multigraph population.

The aforementioned brain multigraph population fusion methods have a major shortcoming: none of them considered how much each *individual* training brain multigraph *influences* the construction of a well-centered, representative, and topologically sound connectional brain template. Especially, since brain multigraph datasets usually come in small sizes, the influence of each brain multigraph is even greater. Quantifying the influence score of each brain multigraph in a fully unsupervised manner and selecting the most influential brain multigraphs to build the training set for CBT estimation is the key to generating a more centered, representative, and topologically sound CBT.

Sample selection methods. Not all training samples may prove beneficial for deep learning models. By strategically selecting a subset of helpful samples (proponents) from the training data, we can potentially enhance the model accuracy. In other words, the overall goal of sample selection methods is to find a subset of the training data such that the trained model using such a subset will result in a minimal loss compared to using the whole training dataset. Without any loss of generalizability, this line of reasoning extends to any set of training data represented by multigraphs.

In their work, Koh and Liang (2017) used influence functions to calculate the impact of training data on a model's prediction by tracking it through the learning algorithm. Essentially, these functions measure how much a test point's loss changes when a model is retrained without a specific training point. Tangentially, a similar paper Wang et al. (2018) used a two-round training, in the first round, they utilized Hessian-vector products to estimate data influence scores and remove 'harmful' training data to find the optimal subset of training samples. In the second round, deep learning models are retrained using this new subset of training samples and results show that network performance boosted computer vision tasks. In another work, Hara et al. (2019) proposed a novel method to infer the influence of data for models trained with stochastic gradient descent (SGD) by retracing the steps of the SGD while incorporating intermediate models computed in each step. Data Shapley is utilized as a metric in Ghorbani and Zou (2019) to evaluate the value of each training point in the model performance. A simple and general method is proposed by Pruthi et al. (2020), to identify the influence of a training data point on a test point and this method approximates the change in loss with first-order approximation using gradients calculated at certain checkpoints of the deep neural network training process. Gaonkar et al. (2021) put forward a novel algorithm for data subset selection and failure prediction for deep learning-based medical image segmentation named 'Eigenrank by committee'.

These studies have shown their success in diverse learning tasks including classification and image segmentation using well-known deep learning networks. However, the effectiveness of sample selection methods in the multigraph population fusion using graph neural networks remains unexplored. Specifically within network neuroscience, the limited availability of labeled clinical data amplifies the necessity for **unsupervised sample influence estimation methods** in the context of CBT learning. We set out to quantify the influence of training multigraphs for the multigraph population fusion task in a *fully unsupervised manner*.

The landscape of connectional brain templates in holistic brain mapping. The connectional brain template encapsulates the key and representative characteristics (i.e., connectivities) of a population of brain networks. We can use a CBT to substantially improve the performance in prediction and classification tasks associated with brain connectomes (Chaari et al., 2023; Pala and Rekik, 2022; Özen et al., 2021; Demirbilek and Rekik, 2023; Gürler et al., 2023; Guvercin et al., 2021; Bayram and Rekik, 2021; Bessadok et al., 2021; Duran et al., 2022). For instance, Demirbilek and Rekik (2023) introduced a novel architecture called Recurrent Multigraph Integrator Network (ReMI-Net) designed to predict population templates at consecutive timepoints from a given single timepoint. ReMI-Net is capable of identifying the atypical connectivity alterations over time to distinguish patients with neurodegenerative disorders with diverse temporally-dynamic patterns. In their recent work, Guvercin et al. (2021) used a representative CBT for one-shot learning, aiming to train a GNN model for brain state classification. This work provided a proof-of-concept of the representation of a single CBT in one-shot brain network classification and regression tasks, thereby lightening the heavy learning of deep learning models by training on one sample (i.e., CBT) instead of all. Pala and Rekik (2022) introduced Multigraph Generator Network (MultigraphGNet), a novel GNN architecture designed to generate brain multigraphs that capture various types of node connectivity from a single brain graph. This architecture includes two learning blocks: a many-to-one GNN model integrating an input population of brain multigraphs into a CBT, and a one-to-many U-Net, which uses the learned CBT in each training step to output the reconstructed input multigraph population. By employing end-to-end training with cyclic loss, the model is able to augment brain multigraphs from a single CBT for boosting downstream classification tasks. Özen et al. (2021) employed CBTs to cost-effectively train a GNN in predicting how brain networks evolve over time, based on a single initial graph. Bayram and Rekik (2021) federated the integration of brain multigraph datasets from various hospitals into a single CBT in a fully privacy-compliant way. Duran et al. (2022) introduced the Dual Hierarchical Integration Network (Dual-HINet), an innovative method to estimate CBTs, offering a more holistic view of brain multigraph populations, such as healthy or atypical ones. Unlike existing methods, Dual-HINet accounts for the hierarchical structure of neural interactions, thereby enhancing our understanding of complex ROI relationships. Bessadok et al. (2021) highlighted that CBTs could serve as powerful graph representations for augmenting brain multigraphs, especially when data is scarce. They accomplish this by using CBTs to generate new connectomic datasets, which aid the learning models in identifying atypical alterations of brain connectivities in disordered populations. We note that all these models have leveraged all existing training data samples for the CBT learning task.

1.2. Contribution

In this work, we propose two major sample influence estimation techniques to determine the *influence* of a training brain multigraph on the target brain multigraph population fusion task using graph neural networks, in *a fully unsupervised manner*: (1) *GraphGradIn*, in which we use gradients w.r.t to GNN weights to approximate the change in the CBT centeredness loss during the *training phase*, whenever the brain multigraph example of interest was utilized and, (2) *GraphTestIn*, in which we drop a training brain multigraph of interest during the CBT refinement step of the *test phase* to trace its influence on the centeredness loss. We assign an influence score to each multigraph that corresponds to the helpfulness level of this data point in the brain multigraph population fusion task. Next, we rebuild the training dataset with a subset that consists of samples with high influence scores (Fig. 1). The idea is to find a subset of the training data such that a trained model using this subset will result in a minimal loss compared to using the whole training dataset. In the next phase, we use the influential training dataset to generate an improved connectional brain template and through extensive experiments on brain multigraph datasets we demonstrate CBT learned with the influential training dataset is enhanced in terms of well-centeredness and discriminativeness, while preserving topological soundness. Additionally, our influence estimation method does not require labeled data; therefore, it is carried out in a fully unsupervised manner.

To summarize, we present two novel unsupervised sample influence estimation techniques, marking this as the first study to incorporate sample selection methods in GNN training for multigraph integration. By identifying the proponent samples for the target integration task in a fully learnable way, we improved the representativeness and efficacy of the GNN-based integration model. Our novel sample selection methods, *GraphGradIn* and *GraphTestIn*, are both grounded in loss-based computations. Both strategies examine how individual data points impact the GNN model learning and performance through their influence on the loss function. Next, using the influence scores, we identify the helpful samples, and we subsequently use these identified helpful samples to form a new refined training dataset. This helps the model learn more centered, discriminative, and topologically sound connectional brain templates. Our work offers promising contributions towards clinical applications, particularly in the domain of biomarker discovery for Alzheimer's disease and autism spectrum disorder, underlying the potential of improved connectional brain templates in advancing neuroscientific research.

The main contributions of our work can be listed as follows:

- We propose *GraphGradIn* (during training phase) or *GraphTestIn* (during test phase) to quantify the influence scores of training brain multigraphs in the target brain multigraph population fusion task using GNN, in a *fully unsupervised manner*.
- We rebuild the influential training dataset using brain multigraph data with high influence scores, retrain the model and generate an improved connectional brain template.
- We conduct extensive experiments on brain multigraph datasets to demonstrate that our new CBT generated by samples with high influence scores is more centered and discriminative compared to the CBT generated by the whole training dataset, and better preserves the complex topology of the target brain multigraph population.
- Finally, we show that learning more centered, discriminative, and topologically sound connectional brain templates of different brain states helps biomarker discovery for Alzheimer's disease and autism spectrum disorder.

2. Proposed methods

In this section, we present our influential data selection methods: (1) *GraphGradIn*, in which we use gradients w.r.t GNN weights, to track the influence of each individual training multigraph on the centeredness loss during the *training phase* and, (2) *GraphTestIn*, in which we exclude a training multigraph out during the refinement step in the *test phase*. Fig. 2 provides an overview of our proposed methods and Table 1 displays the mathematical notations used throughout the paper.

2.1. Tensor representation of brain multigraphs

We represent each brain multigraph by a tensor $\mathcal{Z}_k \in \mathbb{R}^{n_r \times n_r \times n_v}$ (Fig. 2-a) which captures functional, structural, or morphological connectivities between brain regions of interest (ROIs). This tensor is constructed by stacking connectivity matrices for weighted undirected graphs which have n_r nodes (i.e., brain ROIs) for n_v views. Edges that connect the ith and jth ROIs have the size $\mathbf{e}_{ij} \in \mathbb{R}^{n_v \times 1}$ and capture n_v attributes (i.e., types of interactions between two ROIs). In order to eliminate ROI self-connectivities, we set the diagonal entries for the tensor $\mathcal{Z}_k$ to 0. In addition to edge multi-view attributes, GNN layers of DGN (Gurbuz and Rekik, 2020) also take a node attribute matrix $\mathbf{v}_i^0 \in \mathbb{R}^{n_r \times d_0}$ as input. Here, $k \in \{k_0, \ldots, k_{\text{out}}\}$ is the index of a layer in the architecture and d_k is the dimension of the kth layer. We note that, since brain graphs or connectomes conventionally have no node features, we set entries of the node-specific feature vector to identity vector. Our central aim is to improve the performance of integrating the training dataset (i.e., brain multigraph population) $Z = \{\mathcal{Z}_1, \mathcal{Z}_2, \ldots, \mathcal{Z}_N\}$ by selecting the most influential brain multigraphs to build the train set, and to create a population-representative connectional brain template $\mathbf{T} \in \mathbb{R}^{n_r \times n_r}$ that is well-centered, discriminative and topologically sound. Next, we provide an overview of our graph neural network architecture.

Table 1
Mathematical notations.

Notation	Definition
n_r	total number of nodes (region of interests) in a graph
n_v	total number of measurements (network views) for a subject
n_p	number of most influential multigraphs selected for building the training dataset
$\mathcal{Z}$	an arbitrary multigraph's tensor representation $\in \mathbb{R}^{n_r \times n_r \times n_v}$
e_{ij}	multi-edge connecting nodes i and j
F^k	filter-generating network at layer k that maps $\mathbf{e}_{ij}$ to dynamic weights $\Theta_{ij}^k \in \mathbb{R}^{d_k \times d_{k-1}}$
T	connectional brain template
$\mathrm{T}_{\mathcal{Z}}$	connectional brain template generated for sample $\mathcal{Z}$
T_{ref}	refined connectional brain template for training dataset
$\mathbf{v}_i^0$	node attributes matrix $\in \mathbb{R}^{n_r \times d_0}$
ℓ^{snl}	subject normalization loss
$\ell^{snl}(w, \mathcal{Z})$	subject normalization loss calculated for GNN weights w when multigraph $\mathcal{Z}$ is utilized
λ_v	SNL normalization term
ℓ^c	centeredness loss
$\ell^c(w)$	centeredness loss calculated for GNN weights w
ℓ^c_{-z}	centeredness loss excluding multigraph $\mathcal{Z}$
GraphGradIn($\mathcal{Z}$)	GraphGradIn score of multigraph $\mathcal{Z}$
GraphTestIn($\mathcal{Z}$)	GraphTestIn score of multigraph $\mathcal{Z}$
η_t	step-size of the optimizer at iteration t
$\nabla \ell^{snl}(w, \mathcal{Z})$	SNL loss gradient with respect to GNN weights evaluated at w for the training multigraph $\mathcal{Z}$
$\nabla \ell^c(w)$	centeredness loss gradient with respect to GNN weights evaluated at w

2.2. Graph neural network architecture

2.2.1. Training phase

In the development of our methods, *GraphTestIn* and *GraphGradIn*, we employ the DGN framework (Gurbuz and Rekik, 2020), a structure based on a 3-layer Message Passing Neural Network (MPNN). We begin with the training of DGN (Fig. 2-b) which embeds connectivity patterns onto a high-dimensional vector representation for each node in each graph within the given population, namely a node embedding (Fig. 2-b). These embeddings encapsulate all information provided by the multigraphs using edge-conditioned graph convolution operations (Simonovsky and Komodakis, 2017). In each graph convolution layer and for each multigraph connection e_{ij} linking nodes i and j, we construct an edge-specific weight matrix using an edge-conditioned filter learner $F^k : \mathbb{R}^{n_v} \mapsto \mathbb{R}^{d_k \times d_{k-1}}$. In each layer, the model learns a unique filter for each connection while exploiting the cross-view edge features. For MPNNs, the edge-conditioned convolution defines the message passing function M_k as:

$$M_k = F^k\left(\mathbf{e}_{ij}; w^k\right)\mathbf{v}_j^{k-1} + \mathbf{b}^k; \quad F^k\left(\mathbf{e}_{ij}; w^k\right) = \Theta_{ij}^k \tag{1}$$

where $\mathbf{v}_j^k \in \mathbb{R}^{d_k \times 1}$ is the embedding of node j in layer k, $\mathbf{b}^k \in \mathbb{R}^{d_k}$ is the network bias and F^k is filter-generating network that maps $\mathbb{R}^{n_v}$ to $\mathbb{R}^{d_k \times d_{k-1}}$ using weights w^k. Next, the node embedding update function U_k is defined as:

$$U_k = \Theta^k \cdot \mathbf{v}_i^{k-1} + \mathbf{m}_i^k \tag{2}$$

where

$$\mathbf{m}_i^k = \mathrm{AGGR}\left\{M_k\left(\mathbf{v}_i^{k-1}, \mathbf{v}_j^{k-1}, \mathbf{e}_{ij}\right)\right\}_{j \in N(i)} \tag{3}$$

here AGGR is a permutation invariant aggregation function such as mean or max, $\Theta^k \in \mathbb{R}^{d_k \times d_{k-1}}$ is a learnable parameter and $N(i)$ is the neighbors of node i. In this work we used mean aggregation, therefore the operation below is used in each layer l for every node i:

$$\mathbf{v}_i^k = \Theta^k \cdot \mathbf{v}_i^{k-1} + \frac{1}{|N(i)|}\left(\sum_{j \in N(i)} F^k\left(\mathbf{e}_{ij}; w^k\right)\mathbf{v}_j^{k-1}\right) + \mathbf{b}^k. \tag{4}$$

Next, an edge-specific weight matrix Θ_{ij}^k is generated by learning the filtering function F^k for each layer k by optimizing the loss function.

Subject Normalization Loss. DGN takes only one individual multigraph at a time, yet aims to produce a well-centered population representative and topologically sound connectional brain template without having any ground truth template. Therefore, the first step is to generate a single template $\mathbf{T}_{\mathcal{Z}}$ from a single training sample $\mathcal{Z}$ and optimize it by tracing the subject normalization loss (SNL) (Gurbuz and Rekik, 2020). To calculate SNL, the learned CBT $\mathbf{T}_{\mathcal{Z}}$ is compared against a random subset of training multigraphs. By leveraging the SNL loss, we adjust the model weights, ensuring that the CBT derived from a single training sample precisely represents the entire training population. This is facilitated by the random sampling of training subjects, which serves two purposes: it ensures the CBT accurately reflects the population and also acts as a regularizer, reducing the chances of the model overfitting to the target population. Given the generated CBT $\mathbf{T}_{\mathcal{Z}}$ for sample $\mathcal{Z}$ and $\mathcal{X}_n^v$, which is the vth view of the nth random sample, SNL is defined as follows:

$$\ell^{snl} = \sum_{v=1}^{n_v}\sum_{n \in S}\|\mathbf{T}_{\mathcal{Z}} - \mathcal{X}_n^v\|_F \times \lambda_v \tag{5}$$

Here, λ_v is a normalization term defined as:

$$\lambda_v = \frac{\frac{1}{\mu_v}}{\max\left\{\frac{1}{\mu_j}\right\}_{j=1}^{n_v}} \tag{6}$$

where μ_v is the mean of graph connectivity weights. This view-specific normalization weight is used since brain network connectivity distribution and value range might largely vary across the multigraph views.

2.2.2. Test phase

Post-training refinement. In this post-training refinement step, we utilize all subject-biased templates obtained in the first phase to eliminate bias towards any particular subject in the population (Burak Gürbüz and Rekik, 2021). We select the most centered connections by taking the element-wise median of all subject-biased connectional brain templates as follows:

$$\mathbf{T}_{ref} = \mathrm{med}\left\{\mathbf{T}_1, \mathbf{T}_2, \dots, \mathbf{T}_{|T|}\right\} \tag{7}$$

The median operation could also be replaced with other measures such as average or truncated mean, yet, we used the centeredness score to empirically verify that the median is the most suitable for our case. $\mathbf{T}_{ref}$ is the final refined template of the input multigraph population. We calculate the *centeredness loss* by measuring the mean Frobenius distance between the final connectional brain template $\mathbf{T}_{ref}$ and different views of individuals in the test set as follows:

$$\ell^c = \sqrt{\sum_i\sum_j\left|(\mathbf{T}_{ref})_{ij} - (\mathcal{X}_n^v)_{ij}\right|^2}. \tag{8}$$

We hypothesize that optimally selecting a subset of training data is important for the centeredness, representativeness, and topological soundness of the $\mathbf{T}_{ref}$. For this purpose, we propose two sample influence score calculation methods, *GraphGradIn* and *GraphTestIn*, and select the most influential multigraphs to rebuild the train set. We aim to show that using the influential training dataset for DGN training, improves the quality of the learned CBT in terms of centeredness, ability to capture unique traits of populations, and preserves the complex topology of the target multigraph population.

2.3. Influence score calculation

GraphGradIn. We train a GNN with a weight vector $w \in \mathbb{R}^p$ and our training loss function is SNL, denoted as $\ell^{snl} : \mathbb{R}^p \times Z \to \mathbb{R}$. The SNL for a connectional brain template derived from a training multigraph

$\mathcal{Z}$, utilizing a GNN parameterized by a set of weights w, is denoted as $\ell^{snl}(w, \mathcal{Z})$. In the test phase, we use the Frobenius distance measure to obtain the centeredness (see Section 2.2.2) of the learned connectional brain template ℓ^{c}; thus, the centeredness loss of final refined CBT $\mathbf{T}_{ref}$ with a GNN parameterized by weights w is given by $\ell^{c}(w)$. For a set of training multigraph data $Z_{tr} = \{\mathcal{Z}_1, \mathcal{Z}_2, \dots, \mathcal{Z}_n\}$, we train the GNN by adjusting its weight parameters w to minimize the training loss $\sum_{i=1}^{n} \ell^{snl}$ using an iterative optimization technique (e.g. ADAM) which utilizes one training example $\mathcal{Z}_t \in Z_{tr}$ in iteration t and updates the parameter vector from w_t to w_{t+1}. Next, the influence of training example $\mathcal{Z}$ on the centeredness loss $\ell^{c}(w_t)$ at iteration t is defined as:

$$I_{loss} = \sum_{t:\mathcal{Z}_t=\mathcal{Z}} \ell^{c}\left(w_t\right) - \ell^{c}\left(w_{t+1}\right) \tag{9}$$

We can use the first order gradient approximation (Pruthi et al., 2020) to approximately calculate Eq. (9) as follows:

$$\ell^{c}\left(w_{t+1}\right) = \ell^{c}\left(w_t\right) + \nabla \ell^{c}\left(w_t\right) \cdot \left(w_{t+1} - w_t\right) + O\left(\left\|w_{t+1} - w_t\right\|^2\right) \tag{10}$$

Utilizing the training multigraph $\mathcal{Z}$ at iteration t using an iterative optimization technique in training the model, the change in parameters is calculated as follows:

$$w_{t+1} - w_t = -\eta_t \nabla \ell^{snl}\left(w_t, \mathcal{Z}_t\right), \tag{11}$$

where η_t is the step size at iteration t and $\nabla \ell^{snl}\left(w_t, \mathcal{Z}_t\right)$ is the gradient of the ℓ^{snl} w.r.t weight parameters. Ignoring the higher order-term, we end up with the first-order approximation for the change in loss as follows:

$$\ell^{c}\left(w_t\right) - \ell^{c}\left(w_{t+1}\right) \approx \eta_t \nabla \ell^{c}\left(w_t\right) \cdot \nabla \ell^{snl}\left(w_t, \mathcal{Z}_t\right) \tag{12}$$

By summing over all iterations, we get the first-order gradient approximation for the influence of a multigraph $\mathcal{Z}$:

$$I_{FGA} = \sum_{t:\mathcal{Z}_t=\mathcal{Z}} \eta_t \nabla \ell^{c}\left(w_t\right) \cdot \nabla \ell^{snl}\left(w_t, \mathcal{Z}\right) \tag{13}$$

Let us say $w_{t_1}, w_{t_2}, \dots, w_{t_k}$ are the GNN weights at different epochs. At the ith epoch, we can calculate our gradient-based influence score, *GraphGradIn* as:

$$GraphGradIn(\mathcal{Z}) = \sum_{i=1}^{k} \eta_i \nabla \ell^{snl}\left(w_i, \mathcal{Z}\right) \cdot \nabla \ell^{c}\left(w_i\right) \tag{14}$$

GraphGradIn can be calculated by summing the gradients at different epochs if one wants to account for the impact of the training data on various characteristics of the model. In this study, we used only the final epoch to calculate the influence score. After assigning a *GraphGradIn* score to each training brain multigraph, we can sort the samples from the best to the worst scores and select the most influential brain multigraphs to build the training dataset. We will show that using this training subset for the training of our GNN significantly improves the centeredness, discriminativeness, and topological soundness of the learned connectional brain template. Moreover, we do not need multigraph labels to calculate *GraphGradIn*, therefore it is fully unsupervised.

GraphTestIn. Let $\mathbf{T}$ represent the subject-biased connectional brain template and $\mathbf{T}_{\text{ref}} = \text{med}\left\{\mathbf{T}_1, \mathbf{T}_2, \dots, \mathbf{T}_{|T|}\right\}$ indicates the refinement process, in which we select the most centered connections by taking the element-wise median of all subject-biased connectional brain templates. For *GraphTestIn*, during the refinement part of the GNN *test phase*, we exclude a subject-biased connectional brain template, $\mathbf{T}_{\mathcal{Z}}$, associated with a subject of interest $\mathcal{Z}$ to infer its influence on the centeredness loss ℓ^{c} (Fig. 1-D). We denote the final refined connectional brain template generated without the subject $\mathcal{Z}$ as $\mathbf{T}_{\text{ref}}^{-\mathcal{Z}}$ and the centeredness loss calculated using this approach as $\ell^{c}_{-\mathcal{Z}}$. Finally, *GraphTestIn* can be calculated as follows:

$$GraphTestIn(\mathcal{Z}) = \sum_{i=1}^{k} \ell^{c}_{-\mathcal{Z}} - \ell^{c} \tag{15}$$

Table 2
Data characteristics for NC/ASD and AD/LMCI dataset. Each view in the datasets contains 35 nodes, and views are fully connected.

Dataset	NC	ASD	AD	LMCI
Number of subjects	186	155	70	64
Male	147	140	32	32
Female	39	15	38	32
Mean age	15.36	16.92	75.27	72.54
Number of views	6	6	4	4

Similar to *GraphGradIn*, we can use k different weights taken from different epochs and i denotes the ith epoch. In this study, we used only the final epoch to calculate the influence score. We can sort the multigraphs from best to worst using influence scores calculated by *GraphTestIn*, and select the most influential samples to rebuild the training dataset. We do not need graph labels to calculate Eq. (15), therefore it is also a fully unsupervised method.

Remark. *GraphTestIn* can also be applied to CBT generation methods that do not use GNNs such as Wang et al. (2014) since we can exclude the training brain multigraph $\mathcal{Z}$ during the graph fusion process, and generate the final CBT without $\mathcal{Z}$ (i.e. $\mathbf{T}_{\text{ref}}^{-\mathcal{Z}}$). Once we have the $\mathbf{T}_{\text{ref}}^{-\mathcal{Z}}$, *GraphTestIn*($\mathcal{Z}$) can be calculated.

3. Experiments and material

3.1. Models and evaluation datasets

For evaluation, we use two datasets: the first dataset is relatively large in the context of neuroscience research (NC/ASD dataset), it consists of 341 subjects, 186 of them being normal control (NC) and 155 subjects diagnosed with autism spectrum disorder (ASD) collected from the Autism Brain Imaging Data Exchange ABIDE I public dataset (Di Martino et al., 2014). For each subject, there are 6 cortical morphological brain networks derived from the following features: maximum principal curvature, the mean cortical thickness, the mean sulcal depth, average curvature, cortical surface area, and minimum principle area (Soussia and Rekik, 2017, 2018). For both hemispheres, the cortical surface is reconstructed from T1-weighted MRI using the FreeSurfer (Fischl, 2012) pipeline and parcellated into 35 ROIs using Desikan-Killiany (Desikan et al., 2006) atlas and its corresponding brain network is derived by computing the pairwise absolute difference in cortical measurements between pairs of ROIs. The second dataset (AD/LMCI dataset) was collected from the Alzheimer's Disease Neuroimaging Initiative (ADNI) database GO public dataset (Weiner et al., 2015) and includes 67 subjects (35 diagnosed with Alzheimer's diseases (AD) and 32 with Late Mild Cognitive Impairment (LMCI)). For the AD/LMCI dataset, each subject is represented by 4 cortical morphological brain graphs derived from maximum principal curvature, mean cortical thickness, mean sulcal depth, and average curvature measurements. For each hemisphere, the cortical surface is reconstructed from T1-weighted MRI using FreeSurfer (Fischl, 2012) pipeline and parcellated into 35 cortical regions of interest (ROIs) using Desikan-Killiany cortical atlas (Desikan et al., 2006). The corresponding connectivity strength between two ROIs is derived by computing the pairwise absolute difference of their average cortical attribute as introduced in Mahjoub et al. (2018). Data characteristics for the NC/ASD and $AD/LMCI$ populations are given in Table 2.

3.2. Hyperparameters and training

We trained 8 separate models to generate CBTs for the right and left hemispheres of NC, ASD, AD, and LMCI groups. Hyperparameters are set using grid-search, except the n_p number of most influential samples selected for building the training dataset. Since this is a new

Table 3
Hyperparameters and layer settings of the GNN models for ASD/NC and AD/LMCI datasets.

Hyperparameters	NC/ASD	AD/LMCI
No. of Edge-Conditioned Conv. Layers	3	3
Conv. Layer Output Embeddings	32, 32, 64	16, 32, 32
No. of parameters	49568	12496
Type of Edge-Conditioned Conv. Layers	NNConv	NNConv
Activation Function	ReLU	ReLU
Optimizer	Adam	Adam
Learning Rate	0.0006	0.001
No. of Random Samples in SNL loss	10	10
Gradients taken at training epoch	340	340
Training Epochs after rebuilding	800	1500

hyperparameter, we evaluated all models using the top 10% to 40% of training samples with the highest influential scores. We demonstrate how the performance changes with respect to the corresponding n_p and we also show the results for the best n_p selected. Our GNN framework consists of 3 edge-conditioned convolutional layers and each of these layers contains a shallow neural network F^k and each layer is separated by ReLU activation function. Output embeddings of edge-conditioned convolutional layers are 32, 32, 64 (for NC/ASD dataset) or 16, 32, and 32 (for AD/LMCI) dimensions for each ROI in the brain multigraph, respectively. Models are trained using Adam optimizer with a learning rate of 0.0006 with a weight decay of 1 (for NC/ASD dataset) or 0.001 with a weight decay of 0 (for AD/LMCI dataset). The number of random samples in the SNL loss is set to 10. The algorithms are implemented using PyTorch and PyTorch-Geometric (Fey and Lenssen, 2019) frameworks. The message passing convolutional layers used in this work are NNConvs (Gilmer et al., 2017). Our source code is available at https://github.com/basiralab/GraphGradIn.

We split each group into training, validation, and test sets using 5-fold cross-validation. In this work, for our score calculation methods, we have trained the model for 340 epochs for all experiments considering the criteria discussed in Pruthi et al. (2020) that is, where the model has started to learn and at the same time a large loss reduction occurs. The gradients are taken w.r.t weights of the last fully connected layer of DGN. Score calculations are carried out using the validation set, to make sure the test dataset is untouched. After rebuilding the influential dataset, NC/ASD models are trained for 800 epochs and AD/LMCI methods are trained for 1500 epochs and tested using the test set. If there is no decrease in the centeredness loss for more than 60 epochs, early stopping occurs. We summarize the hyperparameters and other layer settings used in our GNN models in Table 3.

3.3. Experiments and benchmarks

We conduct our experiments using SNF (Wang et al., 2014) and the state-of-the-art method DGN (Gurbuz and Rekik, 2020) trained using: **(a)** the entire dataset and **(b)** dataset reconstructed using most influential multigraphs by *GraphGradIn* and *GraphTestIn*, respectively. Note that, SNF operates without a GNN, and the DGN method is the state-of-the-art GNN architecture for multigraph integration (Chaari et al., 2023). Firstly, we analyze the global-graph level similarity by using the centeredness of the estimated CBTs to different views of the test set using Frobenius distance. Next, we investigate the discriminativeness, in which we show how much each CBT encapsulates the most distinctive traits of the input multigraph population. Next, the most discriminative ROIs of typical and atypical CBTs are compared for biomarker discovery of Alzheimer's disease and autism spectrum disorder, respectively. Finally, the estimated CBTs are analyzed at the node level against the "ground truth" population using 3 topological measures. The purpose of the node-level experiments is to assess how much the estimated CBTs preserve the topological properties of the population. In light of our extensive experiments, we provide reliable comparisons for the centeredness, discriminativeness, and topological soundness of the estimated CBTs at the node-level and global-level. To ensure the statistical significance of each experiment, we used Welch's t-test across all data folds.

3.4. Centeredness test

The centeredness score is employed as a measure of how centrally a CBT is positioned within a population of multigraphs by minimizing the distance to all population samples, as documented in studies by Chaari et al. (2021), Dhifallah and Rekik (2019), and Burak Gürbüz and Rekik (2021). In order to evaluate the centeredness loss of the integrated networks (CBTs), we compute the mean Frobenius distance between the estimated CBT and the different views of the tensors (i.e., multigraphs) in the test set for left and right hemispheres of NC/ASD and AD/LMCI datasets, respectively.

3.5. CBT discriminativeness reproducibility and biomarker discovery

A well-representative CBT captures the most distinctive connectivity patterns of a population of brain multigraphs. Discriminative features can be used for downstream classification tasks such as differentiating between a healthy and a disordered brain population. In order to achieve this, we first estimate the CBTs for class-A and class-B populations (e.g., (1) Alzheimer's disease vs late mild cognitive impairment patients and (2) Autism spectrum disorder vs normal control group). To evaluate the reproducibility of the CBT generated by each graph fusion method, we use a randomized 5-fold partition to divide each population into 5 folds. In order to assign a score to discriminativeness to each graph connection we use the absolute difference:

$$\mathbf{D} = \sum_{i,j} \left| \mathbf{A}_{ij} - \mathbf{B}_{ij} \right|, 1 \leq i, j \leq k, \tag{16}$$

where $\mathbf{D} \in \mathbb{R}^{n_r \times n_r}$ matrix contains the absolute differences between all pairs of folds i and j in connectivity weights. Next, we sum the columns of the resulting matrix to get discriminability score vector α, where each ith element corresponds to the ith ROI's assigned score, $\alpha_i = \sum_k \mathbf{D}(i,k), 1 \leq k \leq n_r, k \neq i$. Finally, we can select the top k discriminative ROIs with the highest difference scores.

Additionally, for further assessment of CBT discriminability, we propose to use an independent learner, namely multiple kernel learning (MKL), which aims to identify the most discriminative features for a target classification task disentangling both class-A and class-B populations using support vector machines (SVM). More specifically, for each network view v, we first vectorize the upper triangle of the connection matrix to extract the connection weights of the given population. Next, we concatenate the cross-view edge features e_{ij} and we obtain $k \times 4$ features for AD/LMCI and $k \times 6$ features for NC/ASD populations, respectively. Finally, we train an SVM classifier using the MKL wrapper method on these features to classify brain states. After the identification of the top-k discriminative ROIs by each CBT-based graph fusion method and the MKL-based SVM method, respectively, we report their average overlap accuracies across the 5 cross-validation folds and k values in $\{5, 10, \ldots, 25\}$.

3.6. CBT node-wise similarity comparison

To assess the topological soundness of the learned CBTs, we use node strength (Barrat et al., 2004), PageRank (Xing and Ghorbani, 2004) and second-order centrality measures as they capture different topological properties of graphs. These graph node-wise measures are calculated for each node, and then the node's measure values are compared across learned CBTs.

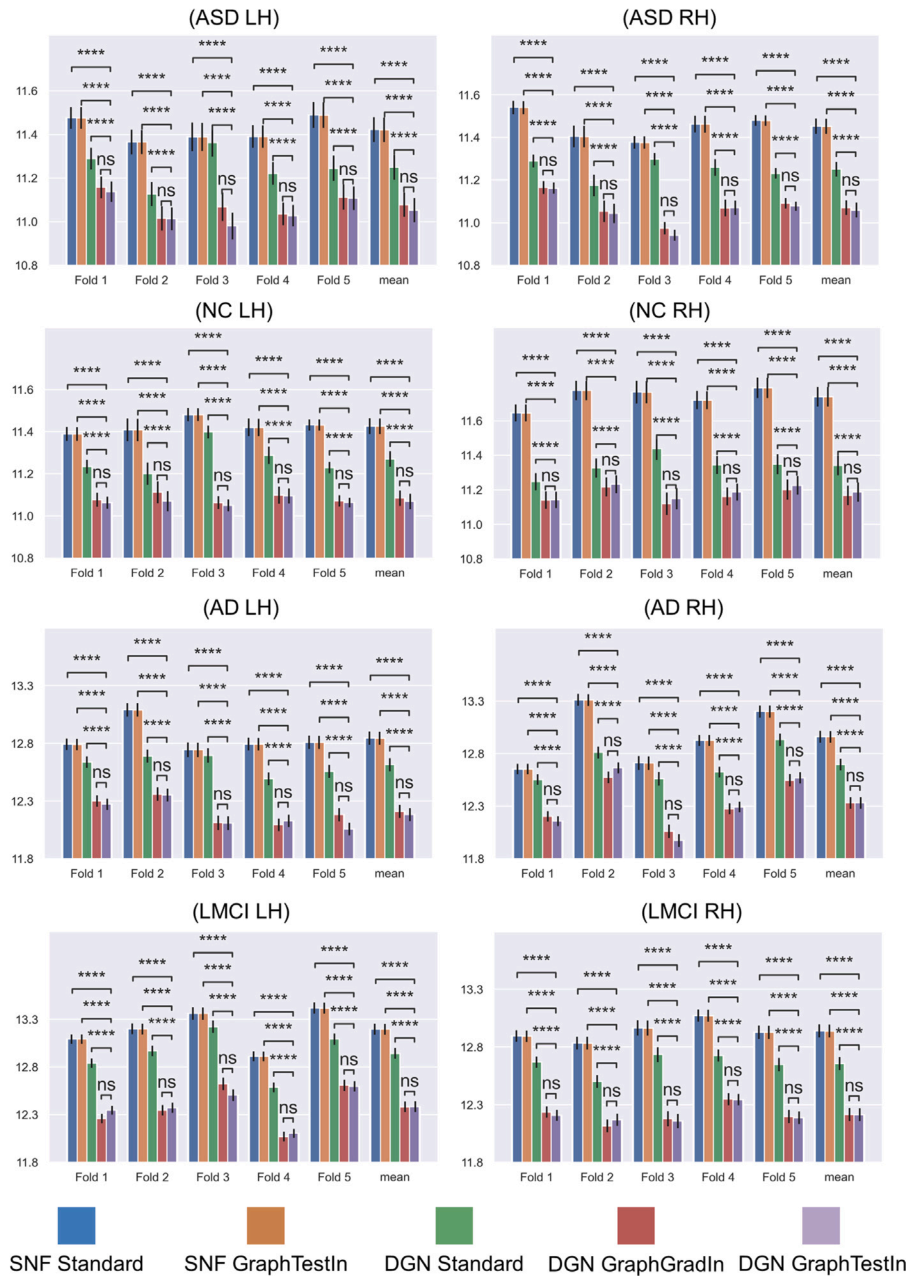

Fig. 3. Centeredness comparison of CBTs generated by SNF (Wang et al., 2014), SNF *GraphTestIn*, DGN (Gurbuz and Rekik, 2020), DGN *GraphGradIn* and DGN *GraphTestIn*. Charts illustrate the mean Frobenius distance between the connectional brain templates estimated using the training sets and networks of the samples in the test set using a 5-fold cross-validation strategy. We report the average distance for each cross-validation fold as well as the average across folds ("Mean" bars on the right). DGN *GraphGradIn* and DGN *GraphTestIn* outperform standard DGN and also SNF with a high statistical significance demonstrated by a Welch's t-test (all $p < 1e\text{-}04$). Also using *GraphTestIn* for SNF has improved compared to standard SNF by a small amount but with a significant statistical significance. ($p < 1e\text{-}04$). The difference between DGN *GraphGradIn* and DGN *GraphTestIn* is not statistically significant ($p > 0.05$). LH: left hemisphere. RH: right hemisphere.

Table 4
Results of CBT centeredness test by DGN, DGN *GraphGradIn*, DGN *GraphTestIn*, SNF and SNF *GraphTestIn*. Values in the table represent the Frobenius distance between the learned CBTs and each network view in the test set. We highlighted the best and second best scorers in bold and underline, respectively. Reconstructing the training dataset using samples with high *GraphGradIn* and *GraphTestIn* influence scores significantly increased the centeredness of the CBT (i.e., closeness to all population network views). Specifically, DGN *GraphGradIn* and DGN *GraphTestIn* outperformed other methods (p-values < 1e-04) and the difference between DGN *GraphGradIn* and DGN *GraphTestIn* is statistically insignificant (p-value > 0.05). Standard deviations of average centeredness values are also given. n_p: number of the most influential samples.

Model variation	Left Hemisphere			
	Average over n_p values		Best n_p selected	
	NC	ASD	NC	ASD
SNF	11.4261 ± 0.01878	11.4221 ± 0.07369	11.4261 ± 0.01878	11.4217 ± 0.07369
SNF *GraphTestIn*	11.4257 ± 0.01880	11.4217 ± 0.07371	11.4256 ± 0.01879	11.4216 ± 0.07370
DGN	11.2699 ± 0.07023	11.2489 ± 0.0778	11.2699 ± 0.07023	11.2489 ± 0.0778
DGN *GraphTestIn*	**11.1315** ± 0.01246,	**11.1099** ± 0.05405,	**11.0844** ± 0.01821	**11.0530** ± 0.0594
DGN *GraphGradIn*	11.1577 ± 0.06269	11.1336 ± 0.0527	11.0683 ± 0.01483	11.0788 ± 0.0524

Model variation	Right Hemisphere			
	Average over n_p		Best n_p selected	
	NC	ASD	NC	ASD
SNF	11.5402 ± 0.05755	11.4528 ± 0.08924	11.5402 ± 0.05755	11.4528 ± 0.08924)
SNF *GraphTestIn*	11.5399 ± 0.05754	11.4524 ± 0.08922	11.5398 ± 0.05755	11.4522 ± 0.08921)
DGN	11.3413 ± 0.06107	11.2505 ± 0.04464	11.3413 ± 0.06107	11.2505 ± 0.04464
DGN *GraphTestIn*	**11.2209** ± 0.0467	11.1487 ± 0.07657	*11.1573* ± 0.03775	**11.0588 ± 0.07099**
DGN *GraphGradIn*	11.2323 ± 0.03823	**11.1096** ± 0.06409	**11.1681** ± 0.03676	11.0706 ± 0.06138

Model variation	Left Hemisphere			
	Average over n_p		Best n_p	
	AD	LMCI	AD	LMCI
SNF	12.8452 ± 0.14500	12.9968 ± 0.16929	12.8452 ± 0.14500	12.9968 ± 0.16929)
SNF *GraphTestIn*	12.8444 ± 0.14496	12.9959 ± 0.16931	12.8440 ± 0.14495	12.9956 ± 0.16933
DGN	12.9420 ± 0.21833	12.6139 ± 0.07876	12.9420 ± 0.21833	12.6139 ± 0.07876
DGN *GraphTestIn*	**12.6809** ± 0.20114	12.4665 ± 0.05357	**12.3838 ± 0.16738**	**12.1831** ± 0.11014
DGN *GraphGradIn*	12.7281 ± 0.20135	**12.4608** ± 0.07245	12.3813 ± 0.21145	12.2091 ± 0.1042

Model variation	Right Hemisphere			
	Average over n_p values		Best n_p selected	
	AD	LMCI	AD	LMCI
SNF	12.9414 ± 0.28203	12.9185 ± 0.08287	12.9414 ± 0.28203	12.9185 ± 0.08287)
SNF *GraphTestIn*	12.9606 ± 0.28201	12.9377 ± 0.08285	12.9603 ± 0.28197	12.9374 ± 0.08283
DGN	12.6988 ± 0.15285	12.6523 ± 0.08046	12.6988 ± 0.15285	12.6523 ± 0.08046
DGN *GraphTestIn*	**12.5532** ± 0.25551	12.4709 ± 0.12350	**12.3314** ± 0.25645	**12.2128** ± 0.06764
DGN *GraphGradIn*	12.5609 ± 0.25267	**12.4607** ± 0.11495	12.3318 ± 0.19900	12.2144 ± 0.07726

Node strength S_{c_i} (Barrat et al., 2004) reflects the importance of node c_i in a graph. S_{c_i} is measured by summing the weights of edges that connect directly the node with its adjacent neighbors:

$$S_{c_i} = \sum_{j}^{N} \mathbf{W}_{ij}, \tag{17}$$

where $\mathbf{W}$ is the weighted graph adjacency matrix.

PageRank (Xing and Ghorbani, 2004) is a measure of importance that can be applied to investigate graph topologies in various domains including biology and neuroscience. We used the power iteration method for calculation and set the damping parameter and maximum iteration to 0.85 and 200, respectively.

Second-order centrality (Kermarrec et al., 2011) provides a value indicating the node's relative importance and relies on a random walk visiting the network in an unbiased manner. For each node, the time elapsed is recorded between visits of that random walk, and the standard deviation (second-order moment) of this return time is computed.

We used centrality measure (CM) distributions which are discrete distributions composed of the aforementioned topological measures calculated for each node. For SNF (Wang et al., 2014) and DGN (Gurbuz and Rekik, 2020) trained with the entire dataset and the dataset build by selecting the most influential multigraphs using $GraphGradIn$ and $GraphTestIn$, distributions are compared including the average distribution as a reference. Average distribution is obtained by averaging the distribution of topological measures (i.e., node strength) of each network view of each testing subject. Note that in the absence of a ground truth CBT, we use the average as a proximal representation of the ground truth. Finally, we compared KL-divergence between CM distributions for each graph integration method with the average distribution over brain ROIs.

4. Results and discussion

4.1. Centeredness test

We evaluate the centeredness of an estimated CBT by measuring its Frobenius distance to each multigraph tensor view of each subject in the test set (Table 4 and Fig. 3). n_p is the number of the most influential samples used to rebuild the training dataset. We chose six values for n_p, ranging from 10% to 40% of the training set size. For example, a fold of the NC dataset has 149 training multigraphs, hence the centeredness scores are averaged across 6 measurements evenly spaced between $n_p = 14$ and $n_p = 59$. Table 4 shows the average of centeredness scores resulting from these 6 different n_p values. Fig. 3 shows the centeredness score for the best n_p selected. Remarkably, both *GraphGradIn* DGN and *GraphTestIn* DGN outperform the standard DGN (Gurbuz and Rekik, 2020), SNF (Wang et al., 2014) and SNF*GraphTestIn* by achieving the lowest Frobenius distance across all four evaluation datasets (ASD/NC

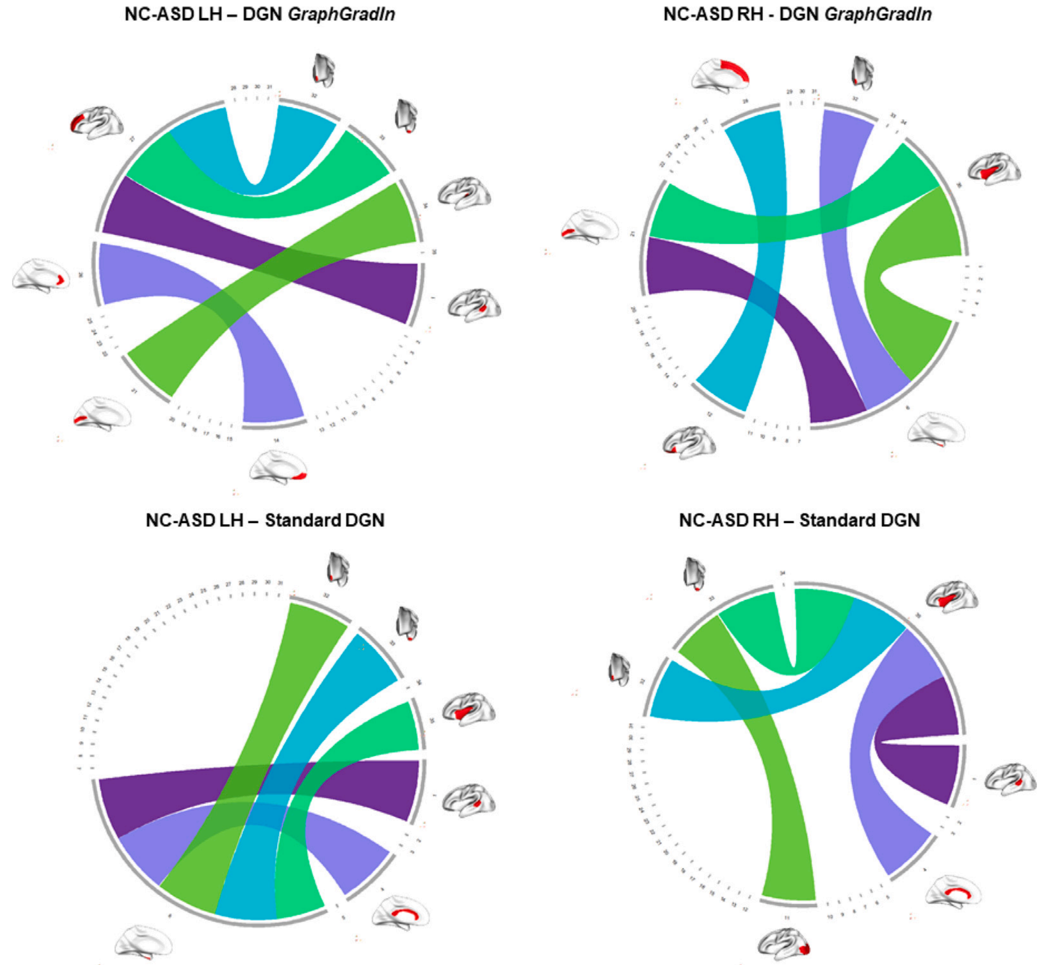

Fig. 4. Circular graphs illustrating the top 5 most discriminative connections that differentiate between two brain states of NC-ASD using training dataset as (i) entire dataset and, (ii) influential dataset reconstructed using *GraphGradIn* influence scores, for both RH and LH. ASD: autism spectrum disorder. NC: normal controls. LH: left hemisphere. RH: right hemisphere.

and AD/LMCI), 5 cross-validation folds and for both hemispheres (LH and RH) according to the centeredness test results given in Table 4 and Fig. 3 (Welch's t-test, p < 1e-04). Additionally, using *GraphTestIn* for SNF improved the learned CBT in terms of centeredness by a small amount, with high statistical significance (p-value < 1e-04). We can conclude that optimally selecting a subset from the dataset to reconstruct the training set greatly contributes to the generation of more centered CBTs.

4.2. Discriminative feature selection test

As a proof of concept of the validity of our hypothesis, we evaluate the discriminative strength of the CBTs estimated by the competing methods using **(i)** the entire training dataset and, **(ii)** a subset of the training samples optimally selected by *GraphGradIn* and *GraphTestIn*, respectively. Specifically, as explained in Section 3.5, we can examine the average overlap rate for the top-$k = 5, 10, \ldots, 25$ ROIs identified by DGN, *GraphGradIn* DGN, *GraphTestIn* DGN, SNF, *GraphTestIn* SNF and a MKL-based SVM classifier. Table 5 shows the averaged overlap rates across the top k discriminative ROIs, with $k = 5, 10, \ldots, 25$. Note that the brain multigraph classification task is challenging and requires carefully designed pre-processing steps and architectures to achieve good accuracy. Remarkably, the usage of our proposed methods to optimally select a subset from the training set for the CBT generation task *boosted the reproducibility in the discriminability of both DGN and SNF* across all datasets, with the exception of the NC-ASD (RH) population.

Table 5
Overlap rate between ROIs selected by SVM binary classification and SNF (Wang et al., 2014), SNF *GraphTestIn*, DGN (Gurbuz and Rekik, 2020), DGN *GraphGradIn* and DGN *GraphTestIn*. Average accuracy across $k = 5, 10, \ldots, 25$ values are presented for classifying AD-LMCI and NC-ASD using the left and right hemispheres features separately (p < 0.05). The standard deviations of average accuracies across k values are also given.

Dataset	Average Accuracy				
	SNF		DGN		
	Standard	*GraphTestIn*	Standard	*GraphGradIn*	*GraphTestIn*
AD-LMCI LH	33.07 ± 2.21	41.58 ± 1.94	48.93 ± 3.21	$\underline{52.13} \pm \underline{2.81}$	61.67 ± 2.96
AD-LMCI RH	39.53 ± 1.32	36.40 ± 1.25	46.13 ± 1.57	$\underline{48.60} \pm \underline{1.34}$	50.73 ± 1.21
NC-ASD LH	40.73 ± 1.84	41.87 ± 1.66	44.73 ± 0.63	57.40 ± 0.84	$\underline{56.60} \pm \underline{0.77}$
NC-ASD RH	48.60 ± 0.92	52.13 ± 0.83	$\underline{55.94} \pm \underline{0.95}$	56.26 ± 0.86	52.60 ± 0.77

These results imply that our proposed sample selection methods improve not only generating more centered connectional brain templates but also significantly better at capturing unique traits of multigraph populations, thereby facilitating downstream classification tasks.

4.3. Biomarker discovery

We further investigate whether using *GraphGradIn* for the CBT generation task affects how the connectivity weights of the learned atypical CBT differ from the learned healthy CBT. In order to recognize and decipher the connectional morphological alterations of brain regions fingerprinting ASD and AD, we identified the top 5 connections with

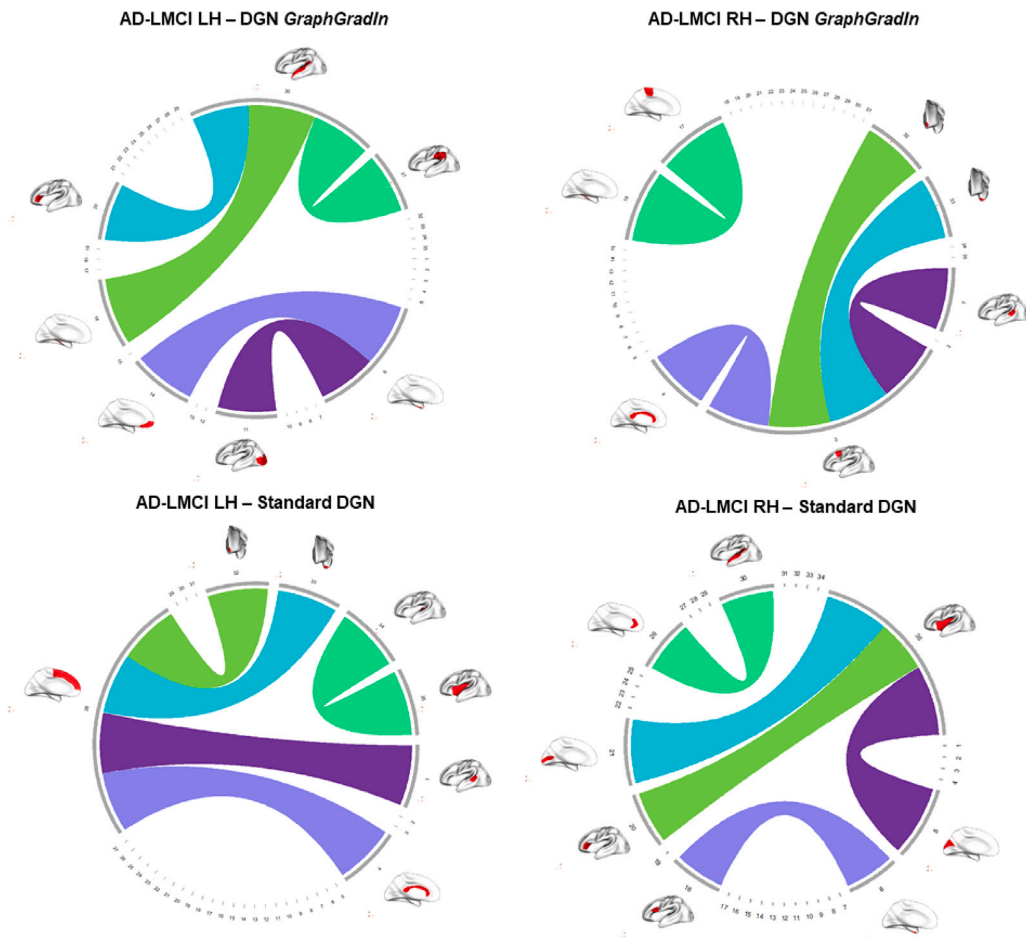

Fig. 5. Circular graphs illustrating the top 5 most discriminative connections that differentiate between two brain states of AD-LMCI using training dataset as (i) entire dataset and, (ii) influential dataset reconstructed using *GraphGradIn* influence scores, for both RH and LH. AD: Alzheimer's disease. LMCI: late mild cognitive impairment. LH: left hemisphere. RH: right hemisphere.

the highest discriminativeness scores (16), using both standard DGN and DGN *GraphGradIn*, respectively (Figs. 4, 5).

Discovered autism spectrum disorder biomarkers. For the standard DGN, the most discriminative connectional morphological biomarkers of the ASD population involved the Frontal pole (FP), Temporal pole (TP), and Corpus Callosum (CC) which fits the existing findings on autism. For instance, Hammond et al. (2008) reported that the right dominant asymmetry of the FPs of boys with ASD could explain their facial asymmetry through the direct effect of brain growth. Additionally, Waiter et al. (2004) reports total grey matter volume was increased in the ASD group relative to the control group, with local volume increases in the FP. PET and voxel-based image analysis revealed a localized dysfunction of the temporal lobes in school-aged children with idiopathic autism (Zilbovicius et al., 2000). Another study Ohnishi et al. (2000), explains the obsessive desire for sameness with altered perfusion in the right medial temporal lobe. In several studies Piven et al. (1997), Frazier and Hardan (2009), the authors detected a significantly smaller size of the body and posterior subregions of the CC in autistic individuals. Using *GraphGradIn* for the CBT generation of DGN revealed an extra region, the rostral anterior cingulate cortex (rACC). In Thakkar et al. (2008), relative to controls, ASD participants showed reduced discrimination between error and correct trials in a rACC region that responds to errors and hyperactive response monitoring in the rACC in ASD that is related to restricted, repetitive behavior and is accompanied by reduced FA in the underlying white matter.

Discovered Alzheimer's disease biomarkers. The most discriminative connectional morphological biomarkers of the AD population involved the middle frontal gyrus (MFG), superior parietal cortex (SPC), and corpus callosum (CC). In Yetkin et al. (2006), subjects with AD underwent fMRI while performing a visual working memory task, and maps of brain activation were obtained. AD groups showed more activation than the controls in the MFG. Another study Jacobs et al. (2012), discusses the parietal lobe involvement in AD. In Janowsky et al. (1996), they showed that AD subjects had smaller CC than healthy elderly subjects or subjects with incipient dementia. Using *GraphGradIn* for the CBT generation by DGN revealed an extra region, namely; the caudal middle frontal gyrus. In Zhao et al. (2015), data revealed that AD subjects had a thinner cortex in the left caudal middle frontal gyrus and the left lateral orbitofrontal gyrus.

4.4. Topologically soundness test

Furthermore, we evaluate the topological soundness of the learned CBTs by comparing the discrepancy of the distribution of various topological measures including (i) PageRank, (ii) node strength, and (iii) second-order centrality between the ground truth brain multigraph population and the learned CBTs. We calculate the ground truth by simply averaging the distribution of the topological measures of each multigraph tensor view for each testing subject. We show the average results across 5 folds for each centrality measure in the form of distribution graphs for ASD/NC (LH, RH) and AD/LMCI (LH, RH), respectively. As displayed in Fig. 6 (ASD/NC) and Fig. 7 (AD/LMCI), standard DGN and *GraphGradIn* DGN shows a striking similarity with the average topology while SNF fails to preserve the data topology.

Second, we compared the learned CBTs by showing Kullback–Leibler (KL) divergence, which measures the dissimilarity between

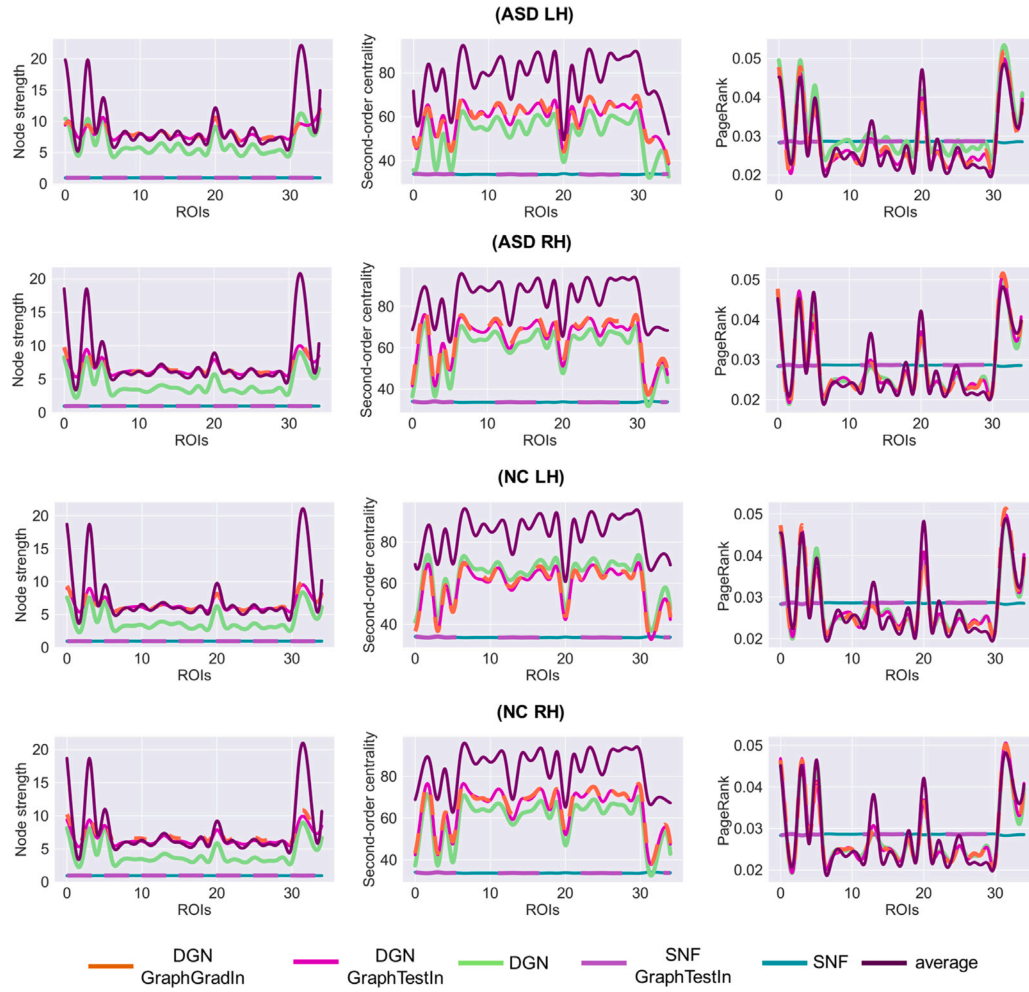

Fig. 6. Average topological distributions across 5-fold cross-validation sets of Node strength (Barrat et al., 2004), Second-order centrality (Kermarrec et al., 2011), PageRank (Xing and Ghorbani, 2004) of templates generated by SNF, SNF *GraphTestIn*, DGN, DGN *GraphGradIn* and DGN *GraphTestIn* against the ground truth distribution of multigraph network for LH and RH of ASD and NC datasets. ASD: autism spectrum disorder. NC: normal controls. LH: left hemisphere. RH: right hemisphere.

the ground truth distribution and each of the distributions obtained from the learned connectional brain templates by each competing method using 5-fold cross-validation. We evaluated the performance of the graph fusion methods based on the lowest value of the average KL-divergence distribution and its standard deviation over all combinations of 5 sub-populations (i.e., folds). A small divergence implies a similar distribution. Fig. 8 shows that DGN *GraphGradIn* and DGN *GraphTestIn* outperform the standard DGN on both ASD/NC and AD/LMCI datasets, across topological measures (Welch's t-test $p < 1e\text{-}04$), excluding node strength (AD/LMCI dataset). Also, the difference between DGN *GraphGradIn* and DGN *GraphTestIn* is not statistically significant.

In summary, through extensive experiments, we showed that the performance of the learned CBTs generated by DGN *GraphGradIn* and DGN *GraphTestIn* improved in terms of estimating the most centered templates and encapsulating the most unique traits of a population of brain multigraph networks while preserving the complex topology of the population. Moreover, we demonstrated that the DGN *GraphGradIn* and DGN *GraphTestIn*-CBTs have revealed a set of biomarkers for Alzheimer's disease, late mild cognitive impairment, and autism spectrum disorder.

5. Conclusion

In this study, we proposed *GraphGradIn* and *GraphTestIn*, to quantify the influence of a training brain multigraph on the learning of a connectional brain template that fingerprints a population of brain multigraphs. We assigned a score to each training multigraph and selected the most influential data samples to build the training dataset, which resulted in a more centered, representative, and topologically sound connectional brain template. We showed the use of our method by learning more centered, discriminative, and topologically sound connectional templates of different brain states for biomarker discovery for Alzheimer's disease and autism spectrum disorder. Both *GraphGradIn* and *GraphTestIn* influence scores are calculated *in a fully unsupervised manner*. Moreover, our methods are generic, both can be computed during the training or test stages of any GNN structure with multigraph inputs. We introduced a prime GNN-based unsupervised influential sample selection for graph integration and fusion tasks.

Although using both *GraphGradIn* and *GraphTestIn* improved the quality of the estimated holistic CBT from heterogeneous brain multigraph datasets, they have a few limitations that could be overcome in future work. First, *GraphGradIn* and *GraphTestIn* select samples based on the subject normalization loss function, which does not necessarily preserve topology constraints. Even though DGN *GraphGradIn* and DGN *GraphTestIn* preserve the complex topology across different datasets, one can further improve the generated template topology by using a loss function that includes topology constraints such as topology-constrained normalization loss function proposed by Burak Gürbüz and Rekik (2021), for the calculation of *GraphGradIn* and *GraphTestIn*. Second, we evaluated our sample selection methods on static

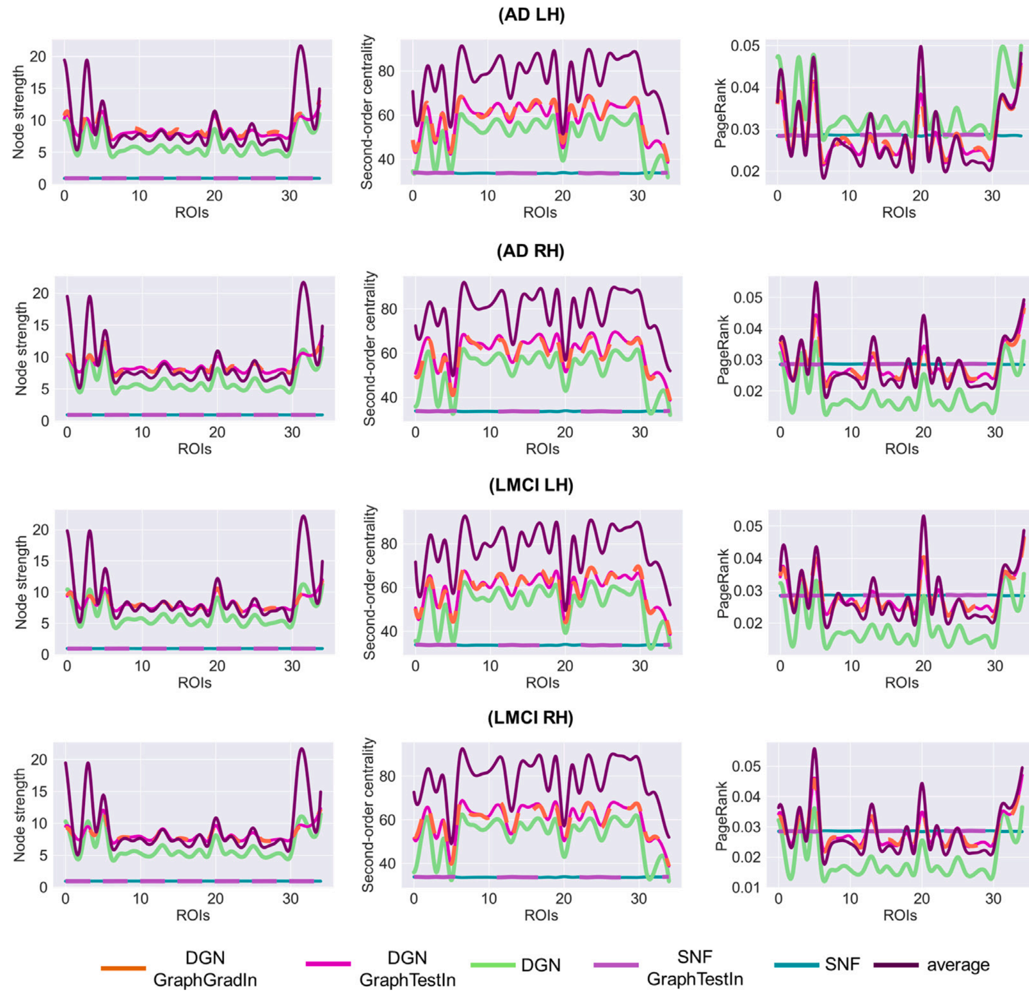

Fig. 7. Average topological distributions across 5-fold cross-validation sets of Node strength (Barrat et al., 2004), Second-order centrality (Kermarrec et al., 2011), PageRank (Xing and Ghorbani, 2004) of templates generated by SNF, SNF *GraphTestIn*, DGN, DGN *GraphGradIn* and DGN *GraphTestIn* against the average distribution of multigraph network for LH and RH of AD and LMCI datasets. AD: Alzheimer's disease. LMCI: late mild cognitive impairment. LH: left hemisphere. RH: right hemisphere.

brain multigraphs (i.e., acquired at a single timepoint). Further investigations are needed to adapt our methods to dynamic multigraph populations (Bessadok et al., 2021; Ghribi et al., 2021). Finally, it is also necessary to investigate how much the computational load of the *GraphGradIn* and *GraphTestIn* methods increases with much larger datasets.

It seems inevitable for high-performing GNN models that predicting connectional brain templates of multigraph populations will become increasingly prevalent and important. Looking at the model through the lens of each training data sample will become a standard part of the toolkit for developing and understanding data-driven models for GNN training.

CRediT authorship contribution statement

Mert Can Kurucu: Methodology, Formal analysis, Validation, Visualization, Writing – original draft, Writing – reviewing & editing. **Islem Rekik:** Conceptualization, Supervision, Methodology, Resources, Writing – reviewing & editing.

Declaration of competing interest

The authors declare that they have no known competing financial interests or personal relationships that could have appeared to influence the work reported in this paper.

Data availability

The authors do not have permission to share data.

Acknowledgments

This work was funded by generous grants from the European H2020 Marie Sklodowska-Curie action (grant no. 101003403, http://basira-lab.com/normnets/) to I.R. and the Scientific and Technological Research Council of Turkey to I.R. under the TUBITAK 2232 Fellowship for Outstanding Researchers (no. 118C288, http://basira-lab.com/reprime/). However, all scientific contributions made in this project are owned and approved solely by the authors.

Data collection and sharing for this project was funded by the Alzheimer's Disease Neuroimaging Initiative (ADNI) (National Institutes of Health Grant U01 AG024904) and DOD ADNI (Department of Defense award number W81XWH-12-2-0012). ADNI is funded by the National Institute on Aging, the National Institute of Biomedical Imaging and Bioengineering, and through generous contributions from the following: AbbVie, Alzheimer's Association; Alzheimer's Drug Discovery Foundation; Araclon Biotech; BioClinica, Inc.; Biogen; Bristol-Myers Squibb Company; CereSpir, Inc.; Cogstate; Eisai Inc.; Elan Pharmaceuticals, Inc.; Eli Lilly and Company; EuroImmun; F. Hoffmann-La Roche Ltd and its affiliated company Genentech, Inc.; Fujirebio; GE Healthcare; IXICO Ltd.; Janssen Alzheimer Immunotherapy Research & Development, LLC.; Johnson & Johnson Pharmaceutical Research

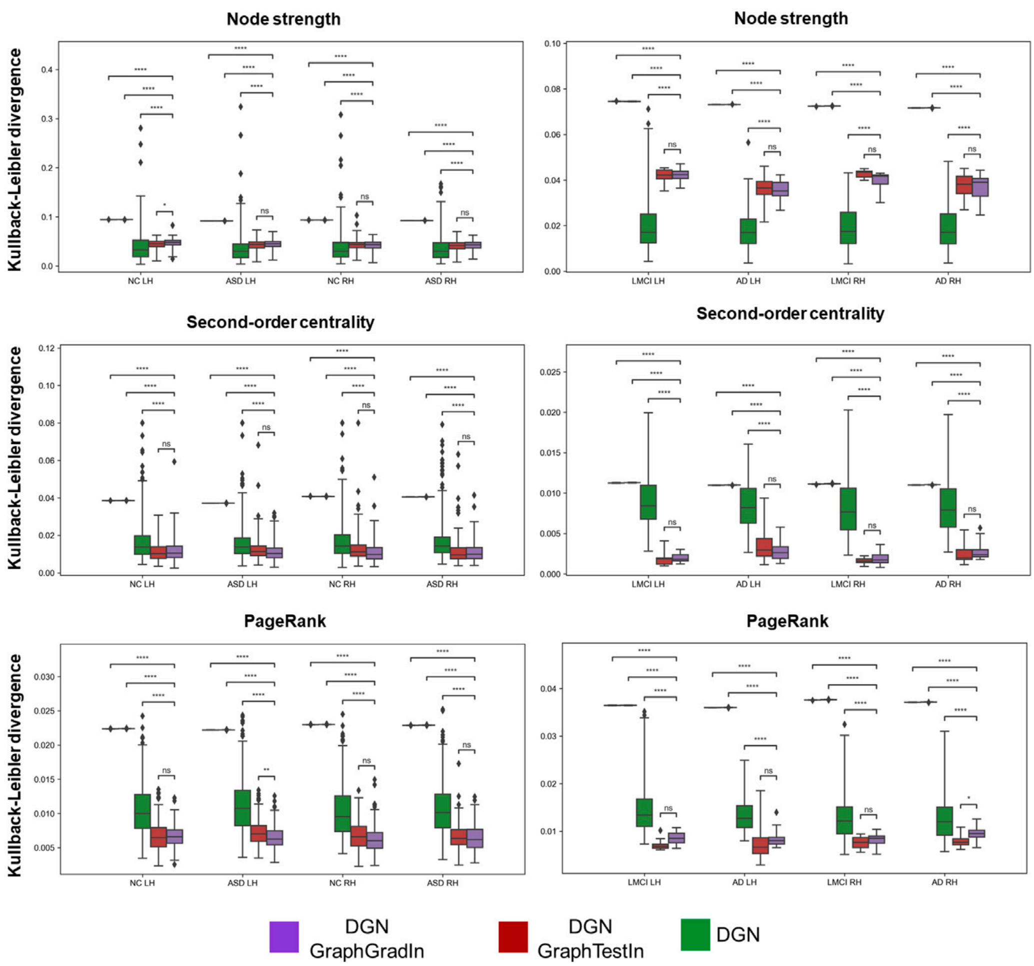

Fig. 8. Average of Kullback–Leibler divergence distribution across 5-fold cross-validation set between average population distribution and average topological distributions of the estimated connectional brain templates generated by SNF (Wang et al., 2014), SNF *GraphTestIn*, DGN (Gurbuz and Rekik, 2020), DGN *GraphGradIn* and DGN *GraphTestIn*.

& Development LLC.; Lumosity; Lundbeck; Merck & Co., Inc.; Meso Scale Diagnostics, LLC.; NeuroRx Research; Neurotrack Technologies; Novartis Pharmaceuticals Corporation; Pfizer Inc.; Piramal Imaging; Servier; Takeda Pharmaceutical Company; and Transition Therapeutics. The Canadian Institutes of Health Research is providing funds to support ADNI clinical sites in Canada. Private sector contributions are facilitated by the Foundation for the National Institutes of Health (www.fnih.org). The grantee organization is the Northern California Institute for Research and Education, and the study is coordinated by the Alzheimer's Therapeutic Research Institute at the University of Southern California. ADNI data is disseminated by the Laboratory for Neuro Imaging at the University of Southern California.

References

Barrat, A., Barthelemy, M., Pastor-Satorras, R., Vespignani, A., 2004. The architecture of complex weighted networks. Proc. Natl. Acad. Sci. 101 (11), 3747–3752. http://dx.doi.org/10.1073/pnas.0400087101.

Bayram, H.C., Rekik, I., 2021. A federated multigraph integration approach for connectional brain template learning. In: Syeda-Mahmood, T., Li, X., Madabhushi, A., Greenspan, H., Li, Q., Leahy, R., Dong, B., Wang, H. (Eds.), Multimodal Learning for Clinical Decision Support. Springer International Publishing, Cham, pp. 36–47.

Bessadok, A., Mahjoub, M.A., Rekik, I., 2021. Graph neural networks in network neuroscience. arXiv preprint arXiv:2106.03535.

Bronstein, M.M., Bruna, J., LeCun, Y., Szlam, A., Vandergheynst, P., 2017. Geometric deep learning: Going beyond euclidean data. IEEE Signal Process. Mag. 34 (4), 18–42. http://dx.doi.org/10.1109/MSP.2017.2693418.

Bullmore, E.T., Bassett, D.S., 2011. Brain graphs: Graphical models of the human brain connectome. Ann. Rev. Clin. Psychol. 7 (1), 113–140. http://dx.doi.org/10.1146/annurev-clinpsy-040510-143934.

Bullmore, E., Sporns, O., 2009. Complex brain networks: graph theoretical analysis of structural and functional systems. Nat. Rev. Neurosci. 10 (3), 186–198. http://dx.doi.org/10.1038/nrn2575.

Burak Gürbüz, M., Rekik, I., 2021. MGN-Net: A multi-view graph normalizer for integrating heterogeneous biological network populations. Med. Image Anal. 71, 102059. http://dx.doi.org/10.1016/j.media.2021.102059.

Chaari, N., Akdağ, H.C., Rekik, I., 2021. Estimation of gender-specific connectional brain templates using joint multi-view cortical morphological network integration. Brain Imaging Behav. 15 (4), 2081–2100. http://dx.doi.org/10.1007/s11682-020-00404-5.

Chaari, N., Akdağ, H.C., Rekik, I., 2023. Comparative survey of multigraph integration methods for holistic brain connectivity mapping. Med. Image Anal. 85, 102741. http://dx.doi.org/10.1016/j.media.2023.102741.

De Vico Fallani, F., Richiardi, J., Chavez, M., Achard, S., 2014. Graph analysis of functional brain networks: practical issues in translational neuroscience. Philos. Trans. R. Soc. B 369 (1653), 20130521. http://dx.doi.org/10.1098/rstb.2013.0521.

Demirbilek, O., Rekik, I., 2021. Recurrent multigraph integrator network for predicting the evolution of population-driven brain connectivity templates. In: de Bruijne, M., Cattin, P.C., Cotin, S., Padoy, N., Speidel, S., Zheng, Y., Essert, C. (Eds.), Medical Image Computing and Computer Assisted Intervention. MICCAI 2021, In: Lecture Notes in Computer Science, Springer International Publishing, Cham, pp. 584–594. http://dx.doi.org/10.1007/978-3-030-87234-2_55.

Demirbilek, O., Rekik, I., 2023. Predicting the evolution trajectory of population-driven connectional brain templates using recurrent multigraph neural networks. Med. Image Anal. 83, 102649. http://dx.doi.org/10.1016/j.media.2022.102649.

Desikan, R.S., Segonne, F., Fischl, B., Quinn, B.T., Dickerson, B.C., Blacker, D., Buckner, R.L., Dale, A.M., Maguire, R.P., Hyman, B.T., Albert, M.S., Killiany, R.J., 2006. An automated labeling system for subdividing the human cerebral cortex on MRI scans into gyral based regions of interest. NeuroImage 31 (3), 968–980. http://dx.doi.org/10.1016/j.neuroimage.2006.01.021.

Dhifallah, S., Rekik, I., 2019. Clustering-based multi-view network fusion for estimating brain network atlases of healthy and disordered populations. J. Neurosci. Methods 311, 426–435. http://dx.doi.org/10.1016/j.jneumeth.2018.09.028.

Dhifallah, S., Rekik, I., 2020. Estimation of connectional brain templates using selective multi-view network normalization. Med. Image Anal. 59, 101567. http://dx.doi.org/10.1016/j.media.2019.101567.

Di Martino, A., Yan, C.G., Li, Q., Denio, E., Castellanos, F.X., Alaerts, K., Anderson, J.S., Assaf, M., Bookheimer, S.Y., Dapretto, M., Deen, B., Delmonte, S., Dinstein, I., Ertl-Wagner, B., Fair, D.A., Gallagher, L., Kennedy, D.P., Keown, C.L., Keysers, C., Lainhart, J.E., Lord, C., Luna, B., Menon, V., Minshew, N.J., Monk, C.S., Mueller, S., Müller, R.A., Nebel, M.B., Nigg, J.T., O'Hearn, K., Pelphrey, K.A., Peltier, S.J., Rudie, J.D., Sunaert, S., Thioux, M., Tyszka, J.M., Uddin, L.Q., Verhoeven, J.S., Wenderoth, N., Wiggins, J.L., Mostofsky, S.H., Milham, M.P., 2014. The autism brain imaging data exchange: towards a large-scale evaluation of the intrinsic brain architecture in autism. Mol. Psychiatry 19 (6), 659–667. http://dx.doi.org/10.1038/mp.2013.78.

Duran, F.S., Beyaz, A., Rekik, I., 2022. Dual-HINet: Dual hierarchical integration network of multigraphs for connectional brain template learning. In: Wang, L., Dou, Q., Fletcher, P.T., Speidel, S., Li, S. (Eds.), Medical Image Computing and Computer Assisted Intervention. MICCAI 2022, Springer Nature Switzerland, Cham, pp. 305–314.

Fey, M., Lenssen, J.E., 2019. Fast graph representation learning with PyTorch geometric. arXiv:1903.02428 [cs, stat].

Fischl, B., 2012. FreeSurfer. NeuroImage 62 (2), 774–781. http://dx.doi.org/10.1016/j.neuroimage.2012.01.021.

Frazier, T.W., Hardan, A.Y., 2009. A meta-analysis of the corpus callosum in autism. Biol. Psychiat. 66 (10), 935–941. http://dx.doi.org/10.1016/j.biopsych.2009.07.022.

Gaonkar, B., Beckett, J., Attiah, M., Ahn, C., Edwards, M., Wilson, B., Laiwalla, A., Salehi, B., Yoo, B., Bui, A.A.T., Macyszyn, L., 2021. Eigenrank by committee: Von-Neumann entropy based data subset selection and failure prediction for deep learning based medical image segmentation. Med. Image Anal. 67, 101834. http://dx.doi.org/10.1016/j.media.2020.101834.

Ghorbani, A., Zou, J., 2019. Data Shapley: Equitable valuation of data for machine learning. In: International Conference on Machine Learning. PMLR, (ISSN: 2640-3498) pp. 2242–2251.

Ghribi, O., Li, G., Lin, W., Shen, D., Rekik, I., 2021. Multi-Regression based supervised sample selection for predicting baby connectome evolution trajectory from neonatal timepoint. Med. Image Anal. 68, 101853. http://dx.doi.org/10.1016/j.media.2020.101853.

Gilmer, J., Schoenholz, S.S., Riley, P.F., Vinyals, O., Dahl, G.E., 2017. Neural message passing for quantum chemistry. In: Proceedings of the 34th International Conference on Machine Learning. ICML '17, pp. 1263–1272.

Gurbuz, M.B., Rekik, I., 2020. Deep graph normalizer: A geometric deep learning approach for estimating connectional brain templates. In: Martel, A.L., Abolmaesumi, P., Stoyanov, D., Mateus, D., Zuluaga, M.A., Zhou, S.K., Racoceanu, D., Joskowicz, L. (Eds.), Medical Image Computing and Computer Assisted Intervention. MICCAI 2020, In: Lecture Notes in Computer Science, Springer International Publishing, Cham, pp. 155–165. http://dx.doi.org/10.1007/978-3-030-59728-3_16.

Gürler, Z., Gharsallaoui, M.A., Rekik, I., 2023. Template-based graph registration network for boosting the diagnosis of brain connectivity disorders. Comput. Med. Imaging Graph. 103, 102140. http://dx.doi.org/10.1016/j.compmedimag.2022.102140.

Gürler, Z., Nebli, A., Rekik, I., 2020. Foreseeing brain graph evolution over time using deep adversarial network normalizer. In: Predictive Intelligence in Medicine. Springer International Publishing, Cham, pp. 111–122. http://dx.doi.org/10.1007/978-3-030-59354-4_11.

Guvercin, U., Gharsallaoui, M.A., Rekik, I., 2021. One representative-shot learning using a population-driven template with application to brain connectivity classification and evolution prediction. In: Predictive Intelligence in Medicine. Springer International Publishing, pp. 25–36.

Hammond, P., Forster-Gibson, C., Chudley, A.E., Allanson, J.E., Hutton, T.J., Farrell, S.A., McKenzie, J., Holden, J.J.A., Lewis, M.E.S., 2008. Face–brain asymmetry in autism spectrum disorders. Mol. Psychiatry 13 (6), 614–623. http://dx.doi.org/10.1038/mp.2008.18.

Hara, S., Nitanda, A., Maehara, T., 2019. Data cleansing for models trained with SGD. arXiv:1906.08473 [cs, stat].

He, Y., Evans, A., 2010. Graph theoretical modeling of brain connectivity. Curr. Opin. Neurol. 23 (4), 341–350. http://dx.doi.org/10.1097/WCO.0b013e32833aa567.

Henaff, M., Bruna, J., LeCun, Y., 2015. Deep convolutional networks on graph-structured data. arXiv:1506.05163 [cs].

Hinton, G., Deng, L., Yu, D., Dahl, G.E., Mohamed, A.r., Jaitly, N., Senior, A., Vanhoucke, V., Nguyen, P., Sainath, T.N., Kingsbury, B., 2012. Deep neural networks for acoustic modeling in speech recognition: The shared views of four research groups. IEEE Signal Process. Mag. 29 (6), 82–97. http://dx.doi.org/10.1109/MSP.2012.2205597.

Jacobs, H.I.L., Van Boxtel, M.P.J., Jolles, J., Verhey, F.R.J., Uylings, H.B.M., 2012. Parietal cortex matters in Alzheimer's disease: An overview of structural, functional and metabolic findings. Neurosci. Biobehav. Rev. 36 (1), 297–309. http://dx.doi.org/10.1016/j.neubiorev.2011.06.009.

Janowsky, J.S., Kaye, J.A., Carper, R.A., 1996. Atrophy of the corpus callosum in Alzheimer's disease versus healthy aging. J. Am. Geriatr. Soc. 44 (7), 798–803. http://dx.doi.org/10.1111/j.1532-5415.1996.tb03736.x.

Kermarrec, A.M., Le Merrer, E., Sericola, B., Tredan, G., 2011. Second order centrality: Distributed assessment of nodes criticity in complex networks. Comput. Commun. 34 (5), 619–628. http://dx.doi.org/10.1016/j.comcom.2010.06.007.

Koh, P.W., Liang, P., 2017. Understanding black-box predictions via influence functions. In: International Conference on Machine Learning. PMLR, (ISSN: 2640-3498) pp. 1885–1894.

Lisowska, A., Rekik, I., 2019. Joint pairing and structured mapping of convolutional brain morphological multiplexes for early dementia diagnosis. Brain Connect. 9 (1), 22–36. http://dx.doi.org/10.1089/brain.2018.0578.

Mahjoub, I., Mahjoub, M.A., Rekik, I., 2018. Brain multiplexes reveal morphological connectional biomarkers fingerprinting late brain dementia states. Sci. Rep. 8 (1), 4103. http://dx.doi.org/10.1038/s41598-018-21568-7.

Monti, F., Boscaini, D., Masci, J., Rodolà, E., Svoboda, J., Bronstein, M.M., 2016. Geometric deep learning on graphs and manifolds using mixture model CNNs. arXiv:1611.08402 [cs].

Ohnishi, T., Matsuda, H., Hashimoto, T., Kunihiro, T., Nishikawa, M., Uema, T., Sasaki, M., 2000. Abnormal regional cerebral blood flow in childhood autism. Brain 123 (9), 1838–1844. http://dx.doi.org/10.1093/brain/123.9.1838.

Özen, G., Nebli, A., Rekik, I., 2021. FLAT-net: Longitudinal brain graph evolution prediction from a few training representative templates. In: Rekik, I., Adeli, E., Park, S.H., Schnabel, J. (Eds.), Predictive Intelligence in Medicine. Springer International Publishing, Cham, pp. 266–278.

Pala, F., Rekik, I., 2022. Predicting brain multigraph population from a single graph template for boosting one-shot classification. In: Rekik, I., Adeli, E., Park, S.H., Cintas, C. (Eds.), Predictive Intelligence in Medicine. Springer Nature Switzerland, Cham, pp. 191–202.

Piven, J., Bailey, J., Ranson, B.J., Arndt, S., 1997. An MRI study of the corpus callosum in autism. Am. J. Psychiatry 154 (8), 1051–1056. http://dx.doi.org/10.1176/ajp.154.8.1051.

Pruthi, G., Liu, F., Kale, S., Sundararajan, M., 2020. Estimating training data influence by tracing gradient descent. Adv. Neural Inf. Process. Syst. 33, 19920–19930.

Reijneveld, J.C., Ponten, S.C., Berendse, H.W., Stam, C.J., 2007. The application of graph theoretical analysis to complex networks in the brain. Clin. Neurophysiol. 118 (11), 2317–2331. http://dx.doi.org/10.1016/j.clinph.2007.08.010.

Rekik, I., Li, G., Lin, W., Shen, D., 2017. Estimation of brain network Atlases using diffusive-shrinking graphs: Application to developing brains. In: Niethammer, M., Styner, M., Aylward, S., Zhu, H., Oguz, I., Yap, P.T., Shen, D. (Eds.), Information Processing in Medical Imaging. In: Lecture Notes in Computer Science, Springer International Publishing, Cham, pp. 385–397. http://dx.doi.org/10.1007/978-3-319-59050-9_31.

Simonovsky, M., Komodakis, N., 2017. Dynamic edge-conditioned filters in convolutional neural networks on graphs. In: 2017 IEEE Conference on Computer Vision and Pattern Recognition. CVPR, (ISSN: 1063-6919) pp. 29–38. http://dx.doi.org/10.1109/CVPR.2017.11.

Soussia, M., Rekik, I., 2017. High-order connectomic manifold learning for autistic brain state identification. In: Wu, G., Laurienti, P., Bonilha, L., Munsell, B.C. (Eds.), Connectomics in NeuroImaging. In: Lecture Notes in Computer Science, Springer International Publishing, Cham, pp. 51–59. http://dx.doi.org/10.1007/978-3-319-67159-8_7.

Soussia, M., Rekik, I., 2018. Unsupervised manifold learning using high-order morphological brain networks derived from T1-w MRI for autism diagnosis. Front. Neuroinform. 12, 70.

Sporns, O., 2012. The human connectome: A complex network. Schizophr. Res. Supplement 1 (136), S28. http://dx.doi.org/10.1016/S0920-9964(12)70100-7.

Sutskever, I., Vinyals, O., Le, Q.V., 2014. Sequence to sequence learning with neural networks. In: Advances in Neural Information Processing Systems, Vol. 27. Curran Associates, Inc..

Taigman, Y., Yang, M., Ranzato, M., Wolf, L., 2014. DeepFace: Closing the gap to human-level performance in face verification. In: 2014 IEEE Conference on Computer Vision and Pattern Recognition. pp. 1701–1708. http://dx.doi.org/10.1109/CVPR.2014.220.

Thakkar, K.N., Polli, F.E., Joseph, R.M., Tuch, D.S., Hadjikhani, N., Barton, J.J., Manoach, D.S., 2008. Response monitoring, repetitive behaviour and anterior cingulate abnormalities in autism spectrum disorders (ASD). Brain 131 (9), 2464–2478. http://dx.doi.org/10.1093/brain/awn099.

van den Heuvel, M.P., Sporns, O., 2019. A cross-disorder connectome landscape of brain dysconnectivity. Nat. Rev. Neurosci. 20 (7), 435–446. http://dx.doi.org/10.1038/s41583-019-0177-6.

Van Essen, D.C., Glasser, M.F., 2016. The human connectome project: Progress and prospects. Cerebrum Dana Forum Brain Sci. 2016.

Waiter, G.D., Williams, J.H.G., Murray, A.D., Gilchrist, A., Perrett, D.I., Whiten, A., 2004. A voxel-based investigation of brain structure in male adolescents with autistic spectrum disorder. NeuroImage 22 (2), 619–625. http://dx.doi.org/10.1016/j.neuroimage.2004.02.029.

Wang, T., Huan, J., Li, B., 2018. Data dropout: Optimizing training data for convolutional neural networks. arXiv:1809.00193 [cs].

Wang, B., Mezlini, A.M., Demir, F., Fiume, M., Tu, Z., Brudno, M., Haibe-Kains, B., Goldenberg, A., 2014. Similarity network fusion for aggregating data types on a genomic scale. Nature Methods 11 (3), 333–337. http://dx.doi.org/10.1038/nmeth.2810.

Wang, P.Y., Sapra, S., George, V.K., Silva, G.A., 2021. Generalizable machine learning in neuroscience using graph neural networks. Front. Artif. Intell. 4.

Wang, M., Zheng, D., Ye, Z., Gan, Q., Li, M., Song, X., Zhou, J., Ma, C., Yu, L., Gai, Y., Xiao, T., He, T., Karypis, G., Li, J., Zhang, Z., 2020. Deep graph library: A graph-centric, highly-performant package for graph neural networks. arXiv:1909.01315.

Weiner, M.W., Veitch, D.P., Aisen, P.S., Beckett, L.A., Cairns, N.J., Cedarbaum, J., Donohue, M.C., Green, R.C., Harvey, D., Jack, C.R., Jagust, W., Morris, J.C., Petersen, R.C., Saykin, A.J., Shaw, L., Thompson, P.M., Toga, A.W., Trojanowski, J.Q., 2015. Impact of the Alzheimer's disease neuroimaging initiative, 2004 to 2014. Alzheimer's Dementia 11 (7), 865–884. http://dx.doi.org/10.1016/j.jalz.2015.04.005.

Wu, Z., Pan, S., Chen, F., Long, G., Zhang, C., Yu, P.S., 2021. A comprehensive survey on graph neural networks. IEEE Trans. Neural Netw. Learn. Syst. 32 (1), 4–24. http://dx.doi.org/10.1109/TNNLS.2020.2978386.

Xing, W., Ghorbani, A., 2004. Weighted PageRank algorithm. In: Proceedings. Second Annual Conference on Communication Networks and Services Research. pp. 305–314. http://dx.doi.org/10.1109/DNSR.2004.1344743.

Yetkin, F.Z., Rosenberg, R.N., Weiner, M.F., Purdy, P.D., Cullum, C.M., 2006. FMRI of working memory in patients with mild cognitive impairment and probable Alzheimer's disease. Eur. Radiol. 16 (1), 193–206. http://dx.doi.org/10.1007/s00330-005-2794-x.

Zhang, Z., Cui, P., Zhu, W., 2022. Deep learning on graphs: A survey. IEEE Trans. Knowl. Data Eng. 34 (1), 249–270. http://dx.doi.org/10.1109/TKDE.2020.2981333.

Zhao, H., Li, X., Wu, W., Li, Z., Qian, L., Li, S., Zhang, B., Xu, Y., 2015. Atrophic patterns of the frontal-subcortical circuits in patients with mild cognitive impairment and Alzheimer's disease. PLoS One 10 (6), e0130017. http://dx.doi.org/10.1371/journal.pone.0130017.

Zilbovicius, M., Boddaert, N., Belin, P., Poline, J.-B., Remy, P., Mangin, J.F., Thivard, L., Barthelemy, C., Samson, Y., 2000. Temporal lobe dysfunction in childhood autism: A PET study. Am. J. Psychiatry 157 (12), 1988–1993. http://dx.doi.org/10.1176/appi.ajp.157.12.1988.